

THE ANOMALOUS MAGNETIC MOMENTS OF THE
CHARGED LEPTONS: THE ELECTRON
THE MUON AND THE TAU

By

GUOWEN LI

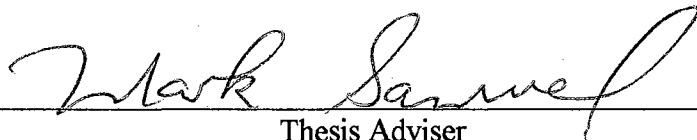
Bachelor of Science
Shanxi University
Taiyuan, Shanxi, P.R.China
1983

Master of Science
Shanxi University
Taiyuan, Shanxi, P.R.China
1986

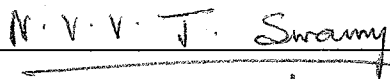
Submitted to the Faculty of the
Graduate College of the
Oklahoma State University
in partial fulfillment of
the requirement for
the Degree of
DOCTOR OF PHILOSOPHY
May, 1994

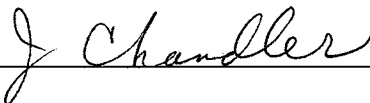
THE ANOMALOUS MAGNETIC MOMENTS OF THE
CHARGED LEPTONS: THE ELECTRON
THE MUON AND THE TAU

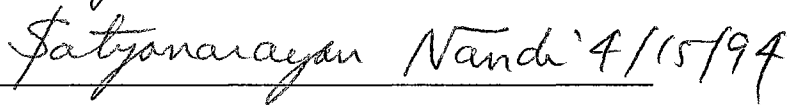
Thesis Approved:

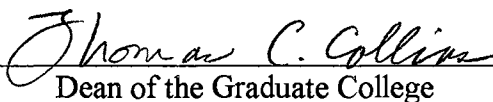


Thesis Adviser









Dean of the Graduate College

ACKNOWLEDGMENTS

First of all I would like to express my sincere gratitude and appreciation to my research advisor, Dr. Mark A. Samuel, for his guidance, support and help throughout the entire research here.

I am thankful to Dr. N. V. V. J. Swamy, Dr. S. Nandi, and Dr. J. P. Chandler for serving on my committee.

I would also like to thank Dr. P. A. Westhaus, Dr. J. Perk, Dr. H. Perk and Dr. J. J. Song for their help during my study here.

Thanks are extended to the Physics Department of Oklahoma State University for the financial support in the form of a teaching assistantship.

Finally I wish to express my sincere appreciation to my parents, my wife and my daughter for their love, patience, understanding and encouragement throughout my study.

TABLE OF CONTENTS

Chapter	Page
I. INTRODUCTION	1
II. ANOMALOUS MAGNETIC MOMENT OF THE ELECTRON	9
III. ANOMALOUS MAGNETIC MOMENT OF THE MUON.....	18
Introduction	18
The Fourth-Order Contribution to $(a_\mu - a_e)$	20
The Sixth-Order Contribution to $(a_\mu - a_e)$	25
The QED Contribution up to Tenth Order	42
Non-QED Contributions and the Muon Anomaly.....	43
IV. ANOMALOUS MAGNETIC MOMENT OF THE TAU.....	46
V. PADÉ APPROXIMATION METHOD	55
General Definition	55
PA Applications to the Anomaly Series.....	58
BIBLIOGRAPHY	66
APPENDIX A - COMPARISON BETWEEN OUR RESULTS AND KINOSHITA'S RESULTS IN THE FOURTH AND SIXTH ORDER QED CONTRIBUTIONS	70
A-1 Comparison in the Fourth Order Contribution.....	70
A-2 Comparison in the Sixth Order Contribution	71
APPENDIX B - PADÉ APPROXIMANT FORTRAN PROGRAM.....	74

LIST OF TABLES

Table	Page
I.	Comparison of $A_2^{(6)}(m_\mu/m_e, \nu p)$ with Kinoshita's Results 35
II.	Padé Approximants to the Series $\ln(1+x)$ with $x = 1$ 60
III.	Padé Approximants to Some Known Series 61
IV.	Padé Approximant to $a_\mu - a_e$ 62
V.	Padé Approximant to a_e 63
VI.	Padé Approximant to a_μ 64
VII.	Padé Approximant to $a_\tau - a_e$ 65
VIII.	Contributions to $A_2^{(6)}(m_\mu/m_e, \gamma\gamma)$ and $A_2^{(6)}(m_\mu/m_e, \nu p)$ 73

LIST OF FIGURES

Figures	Page
1 Quantum Modifications to a Charged Particle	3
2 Lowest-Order Feynman Diagram Describing Scattering of an Electron by an External Magnetic Field.....	4
3 Schematic Diagram Representing an Infinite Set of Feynman Diagrams Contributing to a Particle Anomaly	6
4 Lowest-order (Second-Order) Vertex Diagram Contributing to the Electron Anomaly.....	10
5 Mass-Independent Fourth-Order Vertex Diagrams Contributing to the Electron Anomaly	12
6 Mass-Dependent Fourth-Order Vertex Diagrams Contributing to the Electron Anomaly.....	13
7 Mass-Independent Sixth-Order Diagrams Contributing to a Lepton Anomaly.....	14-15
8 Examples of Mass-Independent Eighth-Order Diagrams Contributing to the Electron Anomaly	17
9 Mass-Independent Sixth-Order Vertex Diagrams Contributing to the Muon Anomaly.....	21
10 Mass-Dependent Fourth-Order Vertex Diagrams Contributing to the Muon Anomaly ((a),(b)) and the Electron Anomaly ((c),(d)).....	22
11 General Case of Mass-Dependent Fourth-Order Vertex Diagram	23
12 Sixth-Order Light-by-Light Scattering Diagram Contributing to $a_{\mu}^{(6)} - a_e^{(6)}$	27

Figures	Page
13 Vacuum-Polarization Diagrams Contributing to $a_{\mu}^{(6)} - a_e^{(6)}$: (a) Second-Order-Electron-Loop-Insertion into a Fourth-Order Muon Vertex. (b) Proper Fourth-Order-Electron-Loop-Insertion into a Second-Order-Muon Vertex. (c) Double-Bubble Second-Order-Electron-Loop-Insertion into a Second-Order Muon Vertex. (d) Mixed-Bubble Second-Order-Loop-Insertion into a Second-Order Muon Vertex.....	28
14 Second-Order τ -Loop-Insertion into a Fourth-Order Muon Vertex.....	37
15 Fourth-Order τ -Loop-Insertion into a Second-Order Muon Vertex.....	38
16 Sixth-Order Mixed Bubble Vertex Diagram Contributing to the Muon Anomaly.....	39
17 General Case of Mass-Dependent Sixth-Order Vertex Diagram.....	40
18 Mass-Dependent Fourth-Order Vertex Diagram Contributing to the Tau Anomaly.....	48
19 Sixth-Order Light-by-Light Scattering Diagrams Contributing to the Tau Anomaly.....	50

CHAPTER I

INTRODUCTION

All the phenomena observed in nature can be attributed to the effects of just four fundamental forces. These are the familiar forces of gravity and electromagnetism, and the not-so-familiar weak and strong forces. The fact that the phenomena occurring in the everyday world can be attributed to just two (gravity and electromagnetism) is true because only these forces have significant effects at observable ranges. The effects of the weak and the strong forces are confined to within, at most, 10^{-15} m of their sources.

Among these four interactions, the electromagnetic interaction, which is described by quantum electrodynamics (QED), is the most understood theory and the comparison between theory and experiment of the anomalous magnetic moment (anomaly) of the electron is one of the most important tests of QED. The “modern” era of quantum electrodynamics dates from the late 1940’s, when the anomalous magnetic moment of the electron [1] and the Lamb shift [2] were first discovered experimentally. The theoretical calculation of the anomalous magnetic moment of electron was first given by Schwinger [3] and since then, both experiment and theory of this field have seen a rapid development. The interplay between theory and experiment has stimulated the evolution of quantum electrodynamics to its present precise form.

The remarkable success of QED lies on its most characteristic feature, renormalizability. Because of this, neither the mass nor the electric charge of a particle is calculable from the theory itself. The most simple quantity which can be computed is the anomalous magnetic moment of a particle. From Dirac theory we know that any Dirac particle has an intrinsic magnetic moment given by

$$\vec{\mu} = -\frac{ge}{2mc}\vec{s} = -\frac{ge}{4mc}\vec{\sigma} \quad (1)$$

with the Landé g factor

$$g = 2. \quad (2)$$

However when the quantum corrections are taken into account, there will be a small deviation from this prediction. In quantum field theory, an electron (or other charged particles) is not just an electron--it can emit a photon, or it can emit a photon that subsequently annihilates into an electron-positron pair, and so on (see Fig. 1). The emitted photon carries off some of the mass of the electron while leaving its charge unaltered. This can then affect the magnetic moment generated by the electron during interactions. The excess, a , is called the anomalous magnetic moment of the particle.

$$a \equiv \frac{g-2}{2}. \quad (3)$$

Then we can write

$$\vec{\mu} = -\frac{ge}{2mc}(1+a)\vec{s}. \quad (4)$$

In order to calculate a , one needs to study the magnetic property of the particle by examining its interaction with a static electromagnetic field $A_\mu(\vec{x})$. In QED, a process can be represented by a set of Feynman diagrams. The vertex of Feynman diagram represents the interaction. Generally the amplitude of interaction is given by

$$T_{fi} = -i \int J_\mu^\beta(x) A^\mu(x) d^4x, \quad (5)$$

where $J_\mu^\beta(x)$ is the transition current of the particle between the initial and the final states.

In the lowest order, as shown in Fig. 2, the amplitude

$$T_{fi} \propto e\bar{u}(P_f)\gamma^\mu u(P_i)A_\mu(\vec{q}), \quad (6)$$

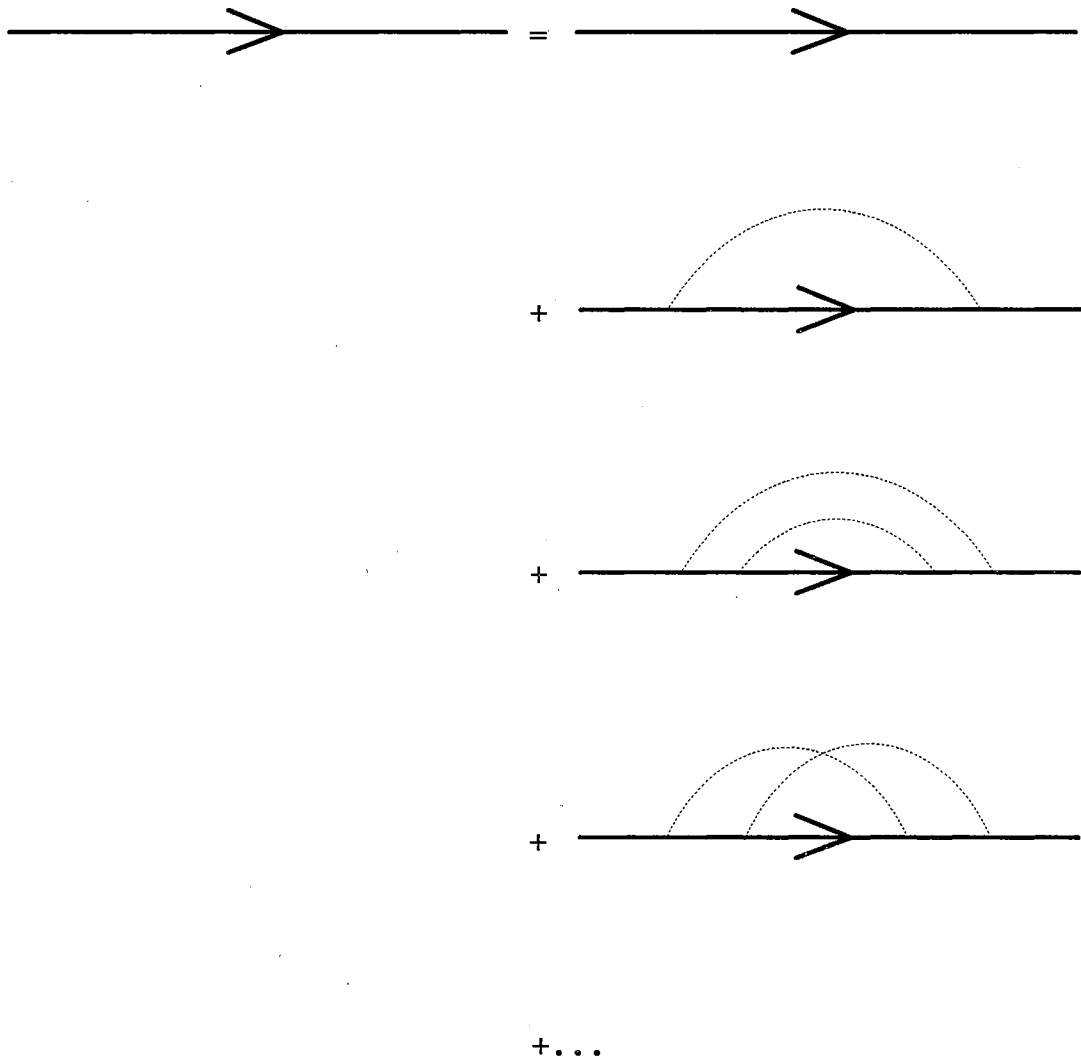


Figure 1. Quantum modifications to a charged particle

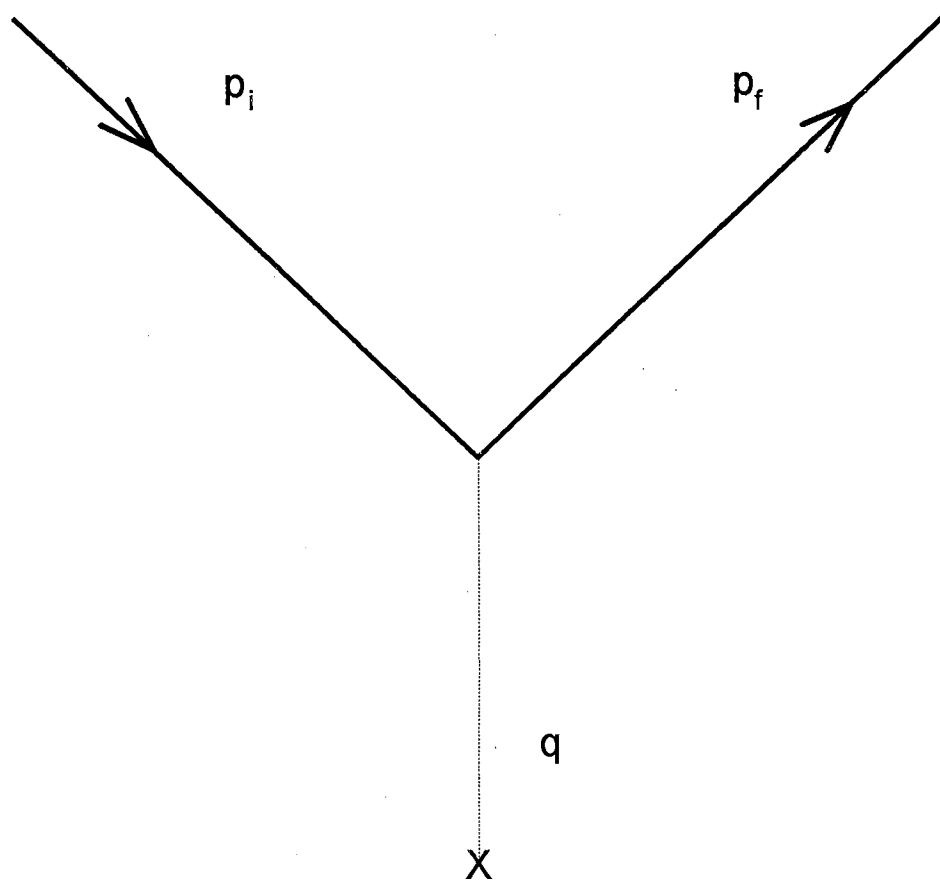


Figure 2. Lowest-order Feynman diagram describing scattering of an electron by an external magnetic field

where

$$A_\mu(\vec{q}) = \frac{1}{(2\pi)^3} \int d^3x A_\mu(\vec{x}) e^{-i\vec{q}\cdot\vec{x}} \quad (7)$$

with $q \equiv P_f - P_i$.

The current can be decomposed into two parts (Golden decomposition):

$$-e\bar{u}(P_f)\gamma^\mu u(P_i) = -\frac{e}{2m}\bar{u}(P_f)(P_f + P_i)^\mu u(P_i) - \frac{ie}{2m}\bar{u}(P_f)\sigma^{\mu\nu}q_\nu u(P_i). \quad (8)$$

The first term corresponds to electric charge interaction and the second term represents the interaction due to the magnetic moment. That is, an electron interacts with an external electromagnetic field via both its charge and its magnetic moment.

For higher order, as shown in Fig. 3, we must consider the interactions with the virtual photon field surrounding the particle. The vertex G , in this case, will be very complicated. The way to handle it is to make the following replacement:

$$\gamma^\mu \rightarrow \gamma^\mu F_1(q^2) + \frac{i}{2m}\sigma^{\mu\nu}q_\nu F_2(q^2), \quad (9)$$

then the current becomes

$$-e\bar{u}(P_f)[\gamma^\mu F_1(q^2) + \frac{i}{2m}\sigma^{\mu\nu}q_\nu F_2(q^2)]u(P_i). \quad (10)$$

Using the Golden decomposition again, we obtain

$$T_{fi} \propto \bar{u}(P_f) \left\{ -\frac{e}{2m}(P_f + P_i)^\mu F_1(q^2) - \frac{ie}{2m}[F_1(q^2) + F_2(q^2)]\sigma^{\mu\nu}q_\nu \right\} u(P_i) A_\mu(x) \quad (11)$$

It is clear that the first term is the charge term if we set $F_1(0) = 1$ and the second term is the magnetic moment term which corresponds to the intrinsic magnetic moment

$$\vec{\mu} = -\frac{ge}{2mc}(1 + F_2(0))\vec{s}. \quad (12)$$

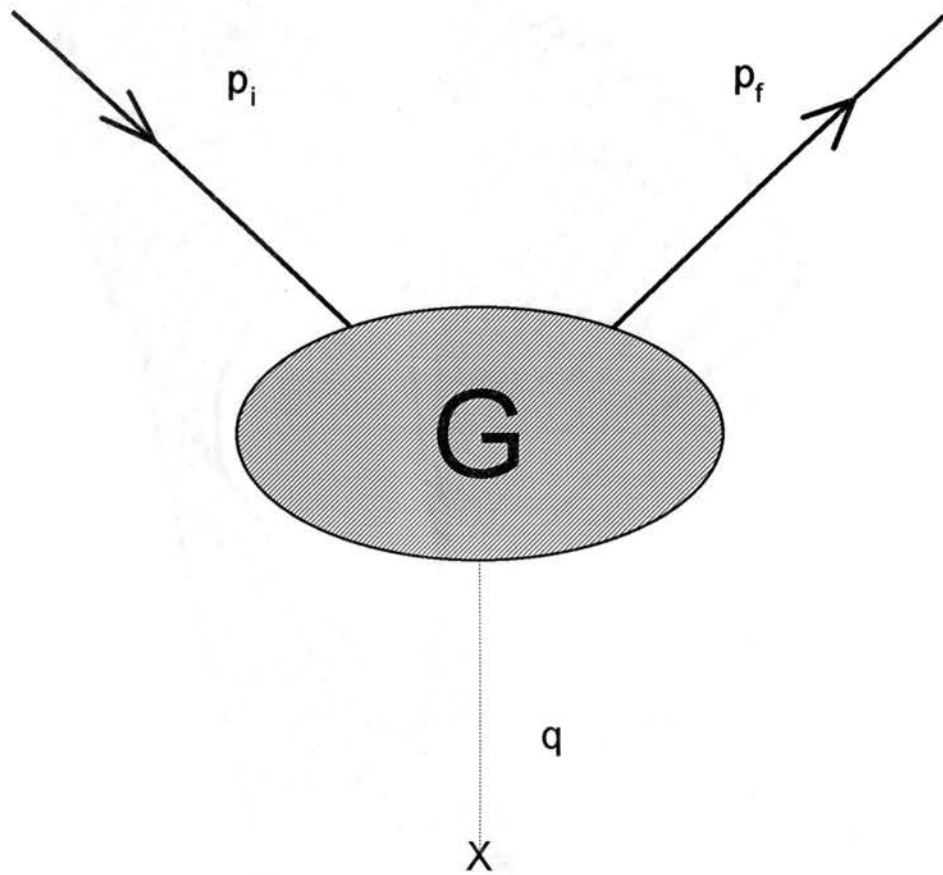


Figure 3. Schematic diagram representing an infinite set of Feynman diagrams contributing to a particle anomaly

Therefore the anomalous magnetic moment is

$$a = F_2(0). \quad (13)$$

In QED, the parameter characterizing each order of perturbation is the fine structure constant $\alpha = e^2 / 4\pi$. The latest value determined from the quantized Hall effect [4] is

$$\alpha^{-1} = 137.0359979(32). \quad (14)$$

The smallness of α is the reason why a perturbative approach has been very successful for QED. As a result, we can express the anomaly in terms of a power series in (α/π) .

Generally the anomalous magnetic moment of a lepton (e, μ , or τ), which is a dimensionless quantity, can be grouped into two parts: mass-independent and mass-dependent parts. The latter can be further divided into two parts, one involving two leptons and the other involving all three leptons. That is, for a lepton with mass m_1 , we can express its anomalous magnetic moment as [5,6]

$$a = A_1 + A_2 \left[\frac{m_1}{m_2} \right] + A_2 \left[\frac{m_1}{m_3} \right] + A_3 \left[\frac{m_1}{m_2}, \frac{m_1}{m_3} \right], \quad (15)$$

where m_2 and m_3 are the masses of the other two leptons. A_1 is the mass-independent part which is the same for all three leptons. $A_2(m_1/m_2)$ and $A_2(m_1/m_3)$ are the mass-dependent part involving two kinds of leptons and $A_3(m_1/m_2, m_1/m_3)$ is the mass-dependent part involving all three leptons.

In Eq. (15), all of the terms can be expanded as a series in (α/π) :

$$A_k = A_k^{(2)} \left[\frac{\alpha}{\pi} \right] + A_k^{(4)} \left[\frac{\alpha}{\pi} \right]^2 + A_k^{(6)} \left[\frac{\alpha}{\pi} \right]^3 + \dots \quad (k = 1, 2, 3). \quad (16)$$

In this way, the anomalous magnetic moment of a lepton can be written as

$$a = A_1^{(2)} \left[\frac{\alpha}{\pi} \right] + \left\{ A_1^{(4)} + A_2^{(4)} \left[\frac{m_1}{m_2} \right] + A_2^{(4)} \left[\frac{m_1}{m_3} \right] \right\} \left[\frac{\alpha}{\pi} \right]^2 + \left\{ A_1^{(6)} + A_2^{(6)} \left[\frac{m_1}{m_2} \right] \right.$$

$$+A_2^{(6)} \left[\frac{m_1}{m_3} \right] + A_3^{(6)} \left[\frac{m_1}{m_2}, \frac{m_1}{m_3} \right] \left\{ \left[\frac{\alpha}{\pi} \right]^3 + \dots \right. \quad (17)$$

We note that, in the second order, we cannot have mass-dependent terms and, in the fourth order, we cannot have the term which involves all three leptons.

In our calculations through this paper, we will use the lepton mass values , $m_\mu = 105.658387(34)$ Mev, $m_e = 0.51099906(15)$ Mev , and $m_\tau = 1776.9(5)$ Mev. We will also use the more accurate value [7] $m_\mu/m_e = 206.768262(30)$ (0.15 ppm).

CHAPTER II

ANOMALOUS MAGNETIC MOMENT OF THE ELECTRON

The anomalous magnetic moment of the electron is the simplest one among the three charged leptons. It involves only pure QED processes and hadronic and weak interactions have no significant contributions to it due to the smallness of its mass. The latest experimental values for the electron and positron anomalies are

$$\begin{aligned} a_{e^-}^{\text{expt}} &= 1159652188.4(4.3) \times 10^{-12}, \\ a_{e^+}^{\text{expt}} &= 1159652187.9(4.3) \times 10^{-12} \end{aligned} \quad (18)$$

obtained by the University of Washington group [8].

Theoretically the anomalous magnetic moment of the electron has been calculated analytically or numerically up to the eighth-order. As we stated in the introduction that the magnetic moment anomaly can be written as a power series in α/π

$$a_e = C_1 \left[\frac{\alpha}{\pi} \right] + C_2 \left[\frac{\alpha}{\pi} \right]^2 + C_3 \left[\frac{\alpha}{\pi} \right]^3 + \dots, \quad (19)$$

where the coefficients C_1, C_2, \dots are finite calculable quantities.

The lowest-order contribution C_1 can be calculated from the Feynman diagram of Fig. 4. The scattering amplitude corresponding to this diagram is given by the Feynman-Dyson rules:

$$\frac{-ie^3}{(2\pi)^4} \int d^4k \frac{1}{k^2} \bar{u}(p') \gamma^\lambda \frac{1}{\not{p}' + \not{k} - m} \gamma^\mu \frac{1}{\not{p} + \not{k} - m} \gamma_\lambda u(p) A_\mu^e(\vec{q}), \quad (20)$$

where $\not{p} = \gamma^\nu p_\nu$. This integration gives

$$C_1 = \frac{1}{2} \quad \text{or} \quad a_e^{(2)} = \frac{\alpha}{2\pi}, \quad (21)$$

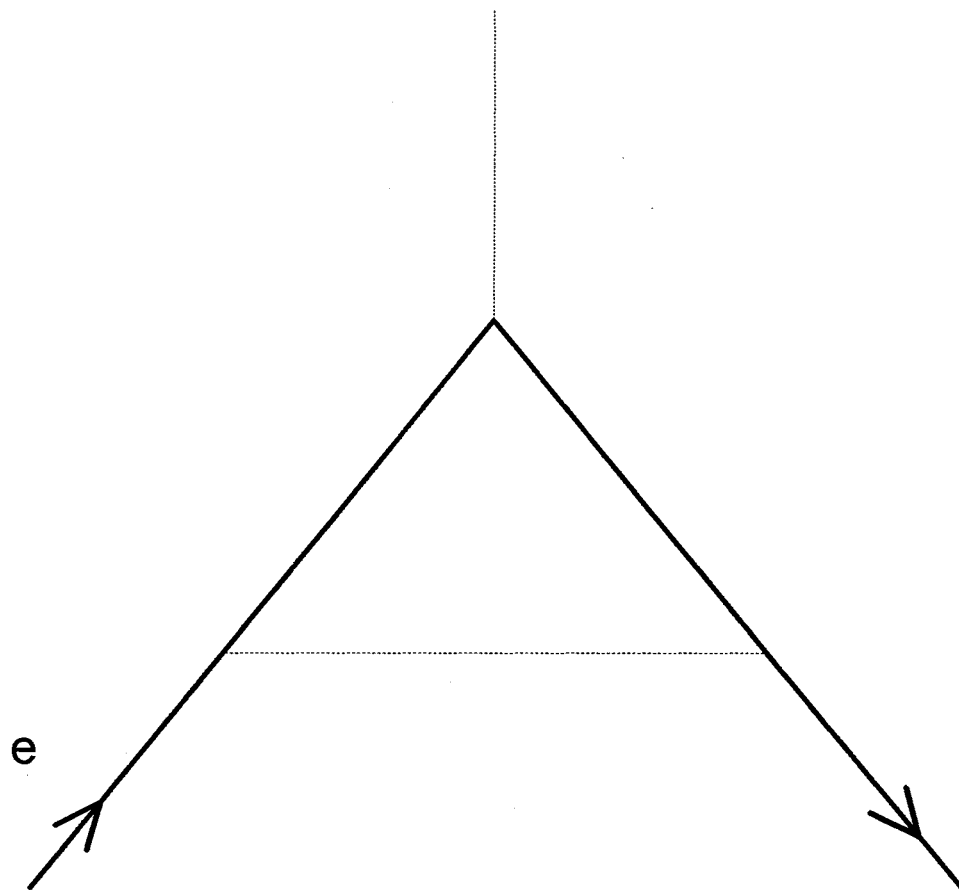


Figure 4. Lowest-order (second-order) vertex diagram contributing to the electron anomaly

which is known as the Schwinger term and was first obtained by Schwinger in 1948.

The major contribution to the fourth order term C_2 comes from the seven mass-independent diagrams as shown in Fig. 5. This contribution was first calculated by Karplus and Kroll in 1949 [9] and revised later by Sommerfield and Petermann [10,11]. The result is rather more complicated than the second order expression. Compared to the rational $1/2$, the transcendentals π^2 , $\pi^2 \log 2$ and $\zeta(3)$ now appear. These represent special values of the dilog $\text{Li}_2(x)$ and the trilog $\text{Li}_3(x)$. More precisely

$$C_2 = \frac{197}{144} + \frac{\pi^2}{12} - \frac{1}{2} \pi^2 \ln(2) + \frac{3}{4} \zeta(3). \quad (22)$$

There are also contributions coming from the mass-dependent diagrams due to the heavy leptons μ and τ as shown in Fig. 6. However, these contributions turn out to be very small at the level of approximation needed and can be left out.

Considering the increase in difficulty between the second and the fourth order it is not surprising that the evaluation of the sixth order contribution is even more difficult. First of all the number of mass-independent graphs is now 72 as shown in Fig. 7 and the complexity of the graphs is such that an analytic evaluation in closed form is extremely difficult for almost all diagrams. The sixth order contribution was first computed numerically by three different groups [12,13,14,15] in 1973-1974. But the estimated error of these numerical integrations exceeded the estimated experimental error of the best measurements. To permit a better test of quantum electrodynamics, it was necessary to improve the numerical accuracy of the calculations. This was achieved primarily over a 10 year period 1972-82, by computing many of the graphs analytically. Some analytic work is still continuing.

Various analytic methods have been developed and successfully applied to the sixth order contribution, such as hyperspherical integrations [16,17,18], Schwinger mass

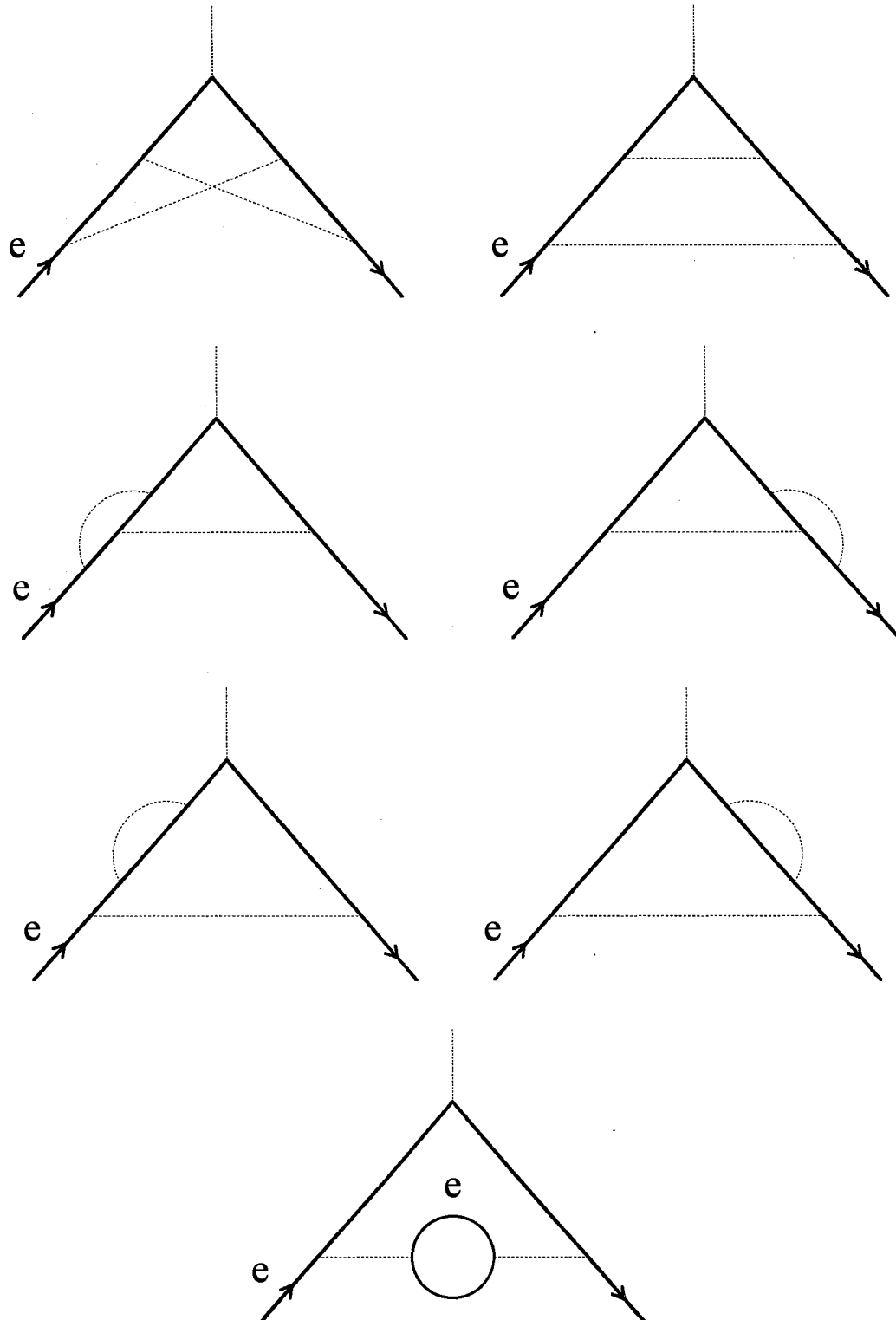


Figure 5. Mass-independent fourth-order vertex diagrams contributing to the electron anomaly

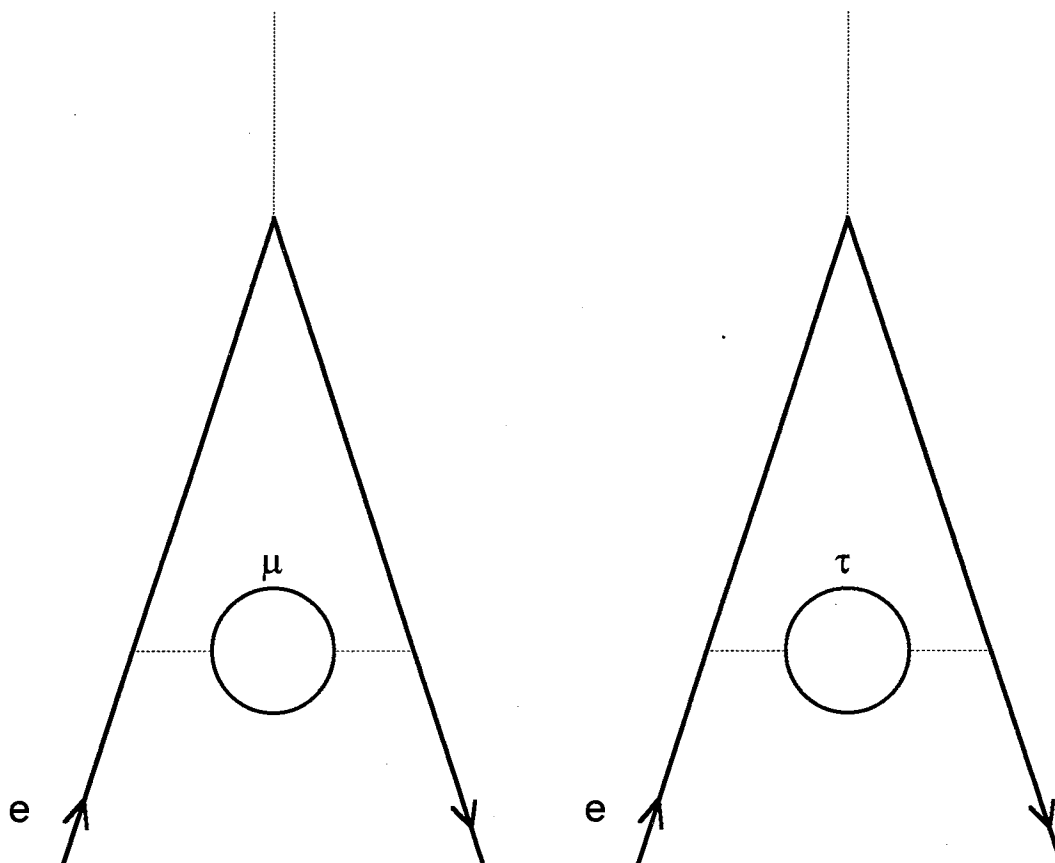


Figure 6. Mass-dependent fourth-order vertex diagrams contributing to the electron anomaly

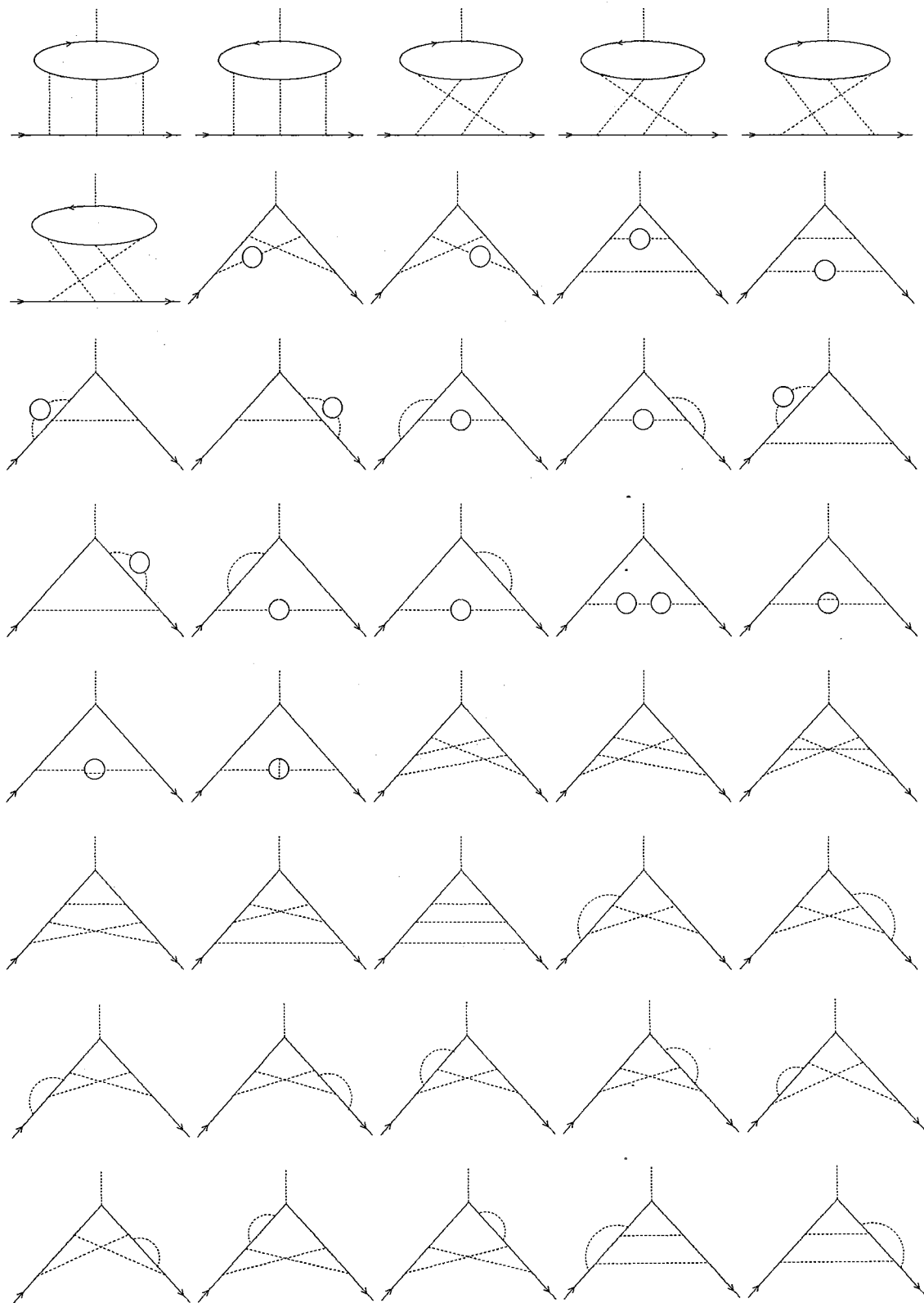


Figure 7. Mass-independent sixth-order diagrams contributing to a lepton anomaly

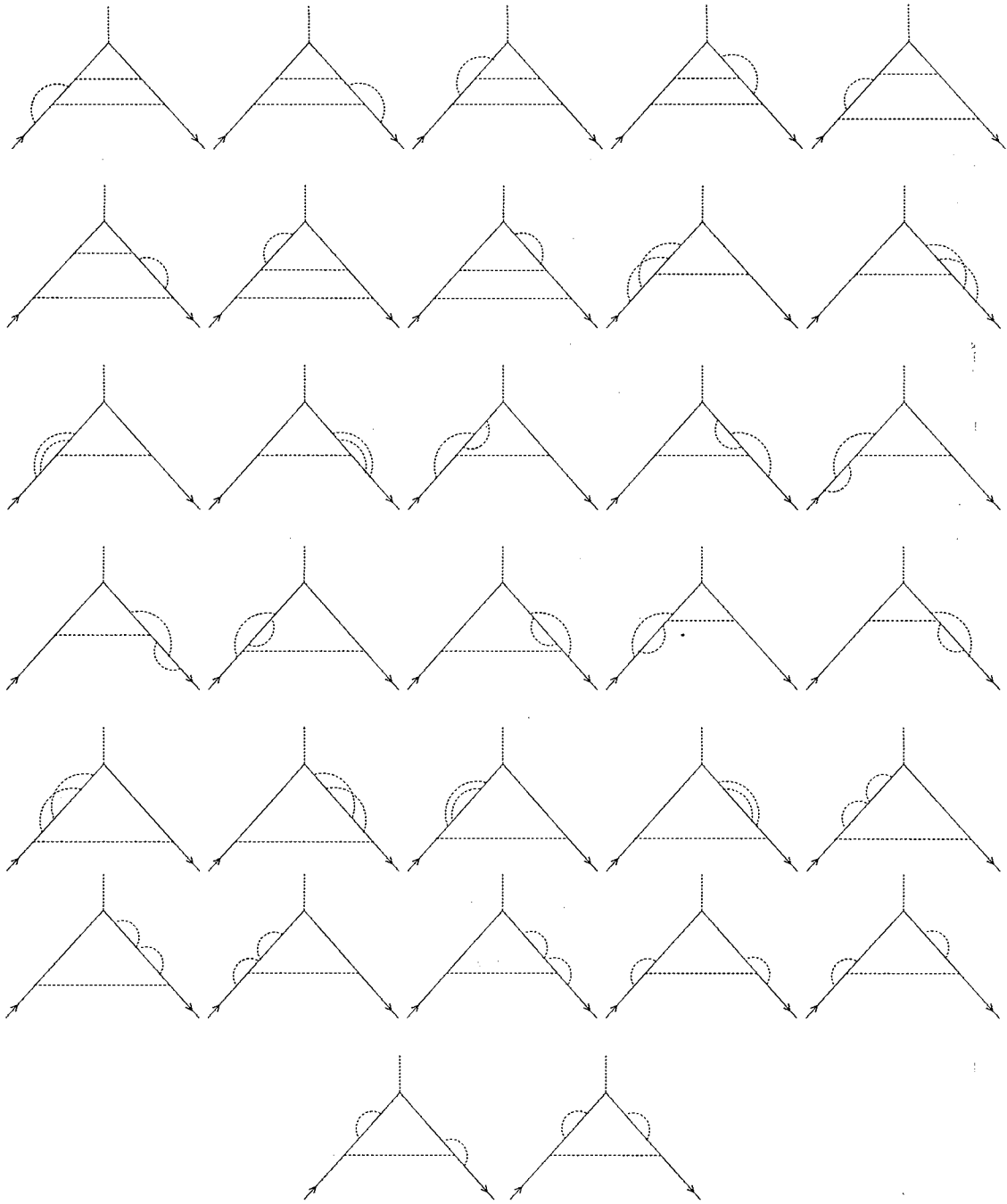


Figure 7. (Continued)

operator [19,20] and dispersion relations [21,22,23,24,25,26,27]. The best value of the sixth order contribution now available is [28]

$$C_3 = 1.17611(42) . \quad (23)$$

The eighth order coefficient C_4 has also been evaluated by Kinoshita and Lindquist [29,30,31,32]. It involves 891 Feynman diagrams and is much more difficult to calculate. The typical diagrams are shown in Fig. 8. The latest value is

$$C_4 = -1.434(138). \quad (24)$$

The tenth order or higher have not been evaluated thus far except for some cases involving multiple insertion of simple vacuum-polarization-loops [33]. An estimate of terms of very large order has been attempted based on the steepest descent method [34]. However, further study is needed to see whether this gives a good asymptotic estimate or not.

To compare with the experimental data, it is also necessary to include the vacuum-polarization contributions of muon, tau and hadron loops as well as the contribution from the electroweak effect. The results are given by [35]

$$\begin{aligned} a_e^{\text{muon}} &= 2.804 \times 10^{-12} , \\ a_e^{\text{tau}} &= 0.010 \times 10^{-12} , \\ a_e^{\text{hadron}} &= 1.6(2) \times 10^{-12} , \\ a_e^{\text{weak}} &= 0.05 \times 10^{-12} . \end{aligned} \quad (25)$$

Collecting all the terms from Eqs. (20), (21), (22), (23), and (24), we obtain the theoretical value

$$a_e^{\text{theory}} = 1159652140(5.3)(4.1)(27.1) \times 10^{-12} , \quad (26)$$

where the first and second uncertainties come from the numerical uncertainties in the sixth order and the eighth order, respectively, while the third one reflects the uncertainty in α .

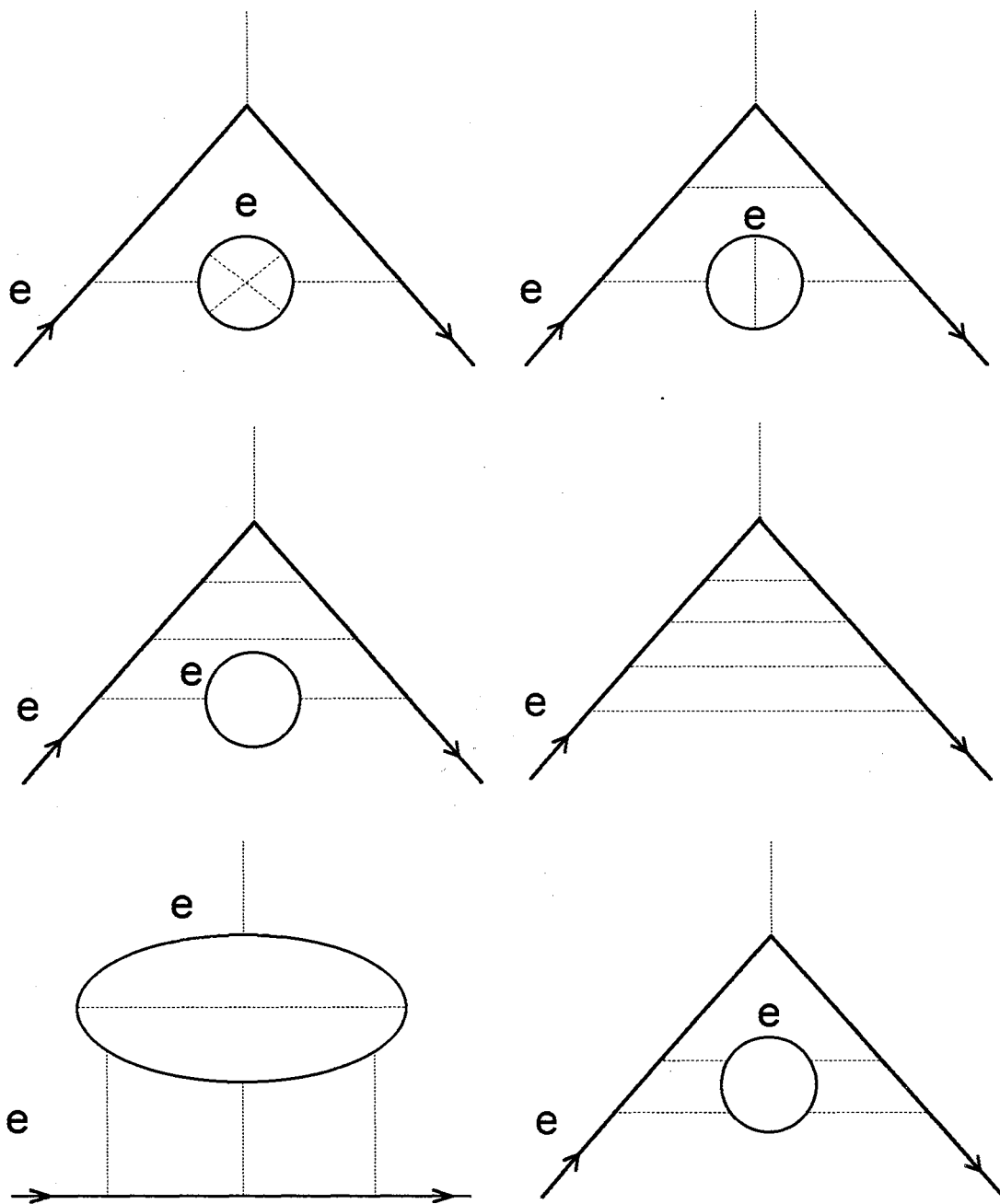


Figure 8. Examples of mass-independent eighth-order diagrams contributing to the electron anomaly

CHAPTER III

ANOMALOUS MAGNETIC MOMENT OF THE MUON

Introduction

Like in the electron case, the comparison between theory and experiment of the muon anomalous magnetic moment also provides an important test of QED. The most accurate measurements now available come from the CERN g-2 experiment [36] in which it was found that

$$a_{\mu^-}^{\text{expt}} = 1165936(12) \times 10^{-9} \text{ (10 ppm)}, \quad (27)$$

$$a_{\mu^+}^{\text{expt}} = 1165910(11) \times 10^{-9} \text{ (10 ppm)}, \quad (28)$$

and the combined result is

$$a_{\mu}^{\text{expt}} = 1165923(8.5) \times 10^{-9} \text{ (7 ppm)}. \quad (29)$$

A new g-2 experiment is planned at Brookhaven National Laboratory (BNL), and an improvement in the accuracy by a factor of about 20 is expected. In order to properly compare experiment and theory one must correspondingly improve the accuracy of the theoretical prediction.

In an heroic feat, Kinoshita, Nizic, Okamoto, and Marciano have calculated the muon anomaly [5,6], a_{μ} , up to the eighth order (the tenth order was also estimated). All of the multidimensional integrals which arise in these calculations were computed numerically. Because of the complexity and the importance of these calculations, they should be independently checked by another group.

In this chapter, we check Kinoshita's results for a_μ in the fourth and sixth order, analytically, by making use of the expansions of $a_\mu^{(4)}$ and $a_\mu^{(6)}$ for large mass ratios $m_\mu/m_e \gg 1$, $m_\tau/m_e \gg 1$, and $m_\tau/m_\mu \gg 1$. We find some small difference with Kinoshita's intermediate results in some cases; however, our final result for a_μ is consistent with his.

In order to get the complete result for a_μ , one must also include the contributions from hadronic and weak effects. However, unlike the QED contributions which can be calculated very accurately, the hadronic contribution is not known very precisely.

One of the goals of the new g-2 experiment at BNL is to measure the weak contribution with some precision. This can be done only if the QED and hadronic contributions are known accurately. Then one would have a very good test of the standard model and possible extensions, such as supersymmetry, composite model, etc. What we propose to do here is to improve and check the QED contributions in fourth and sixth orders.

Since we already know a_e very accurately, the best way to calculate a_μ is to calculate the difference $(a_\mu - a_e)$, from which we can easily find

$$a_\mu = a_e + (a_\mu - a_e). \quad (30)$$

By applying Eq. (17) to the electron and muon, we have

$$\begin{aligned} a_\mu - a_e &= \left\{ A_2^{(4)} \left[\frac{m_\mu}{m_e} \right] + A_2^{(4)} \left[\frac{m_\mu}{m_\tau} \right] - A_2^{(4)} \left[\frac{m_e}{m_\mu} \right] - A_2^{(4)} \left[\frac{m_e}{m_\tau} \right] \right\} \left[\frac{\alpha}{\pi} \right]^2 \\ &+ \left\{ A_2^{(6)} \left[\frac{m_\mu}{m_e} \right] + A_2^{(6)} \left[\frac{m_\mu}{m_\tau} \right] + A_3^{(6)} \left[\frac{m_\mu}{m_e}, \frac{m_\mu}{m_\tau} \right] - A_2^{(6)} \left[\frac{m_e}{m_\mu} \right] - A_2^{(6)} \left[\frac{m_e}{m_\tau} \right] \right. \\ &\quad \left. - A_3^{(6)} \left[\frac{m_e}{m_\mu}, \frac{m_e}{m_\tau} \right] \right\} \left[\frac{\alpha}{\pi} \right]^3 \\ &= (a_\mu - a_e)^{(4)} + (a_\mu - a_e)^{(6)} + \dots \end{aligned} \quad (31)$$

The Fourth-Order Contribution to $(a_\mu - a_e)$

From Eq. (31) we see that the lowest-order contribution to $(a_\mu - a_e)$ is the fourth order contribution

$$(a_\mu - a_e)^{(4)} = \left\{ A_2^{(4)} \left[\frac{m_\mu}{m_e} \right] + A_2^{(4)} \left[\frac{m_\mu}{m_\tau} \right] - A_2^{(4)} \left[\frac{m_e}{m_\mu} \right] - A_2^{(4)} \left[\frac{m_e}{m_\tau} \right] \right\} \left[\frac{\alpha}{\pi} \right]^2. \quad (32)$$

There are a total of nine diagrams contributing to $a_\mu^{(4)}$. Among these, there are seven mass-independent diagrams as shown in Fig. 9 and two mass-dependent diagrams as shown in Figs. 10(a) and 10(b). We have similar diagrams for $a_e^{(4)}$. For the mass-dependent diagrams, we just exchange μ and e , as shown in Figs. 10(c) and 10(d). So there are only four diagrams (Fig. 10) contributing to $(a_\mu - a_e)^{(4)}$: two from $a_\mu^{(4)}$, and two from $a_e^{(4)}$.

Generally for a one-loop insertion diagram as shown in Fig. 11, the contribution can be expressed as the following double integration [37]

$$A_2^{(4)} \left[\frac{M}{m} \right] = \int_0^1 dx \int_0^1 dy \frac{x^2 (1-x) y^2 (1 - \frac{1}{3} y^2)}{x^2 (1-y^2) + 4\lambda^2 (1-x)}, \quad (33)$$

$$\lambda = \frac{m}{M},$$

which has the following exact expression

$$\begin{aligned} A_2^{(4)} \left[\frac{M}{m} \right] = & -\frac{25}{36} - \ln \lambda + \lambda^2 (4 + 3 \ln \lambda) + \frac{\lambda}{2} (1 - 5\lambda^2) \left[\frac{\pi^2}{4} + \ln \lambda \ln \frac{1+\lambda}{1-\lambda} \right. \\ & \left. + f \left(\frac{2}{1-\lambda} \right) - f \left(\frac{2\lambda}{\lambda-1} \right) - 2f(\lambda) + 2f(-\lambda) \right] \\ & + \lambda^4 \left[\frac{\pi^2}{3} - 2 \ln \lambda \ln(1-\lambda) + 2 \ln^2 \lambda - f(\lambda^2) \right], \end{aligned} \quad (34)$$

where $f(x)$ denotes the Spence function [38]

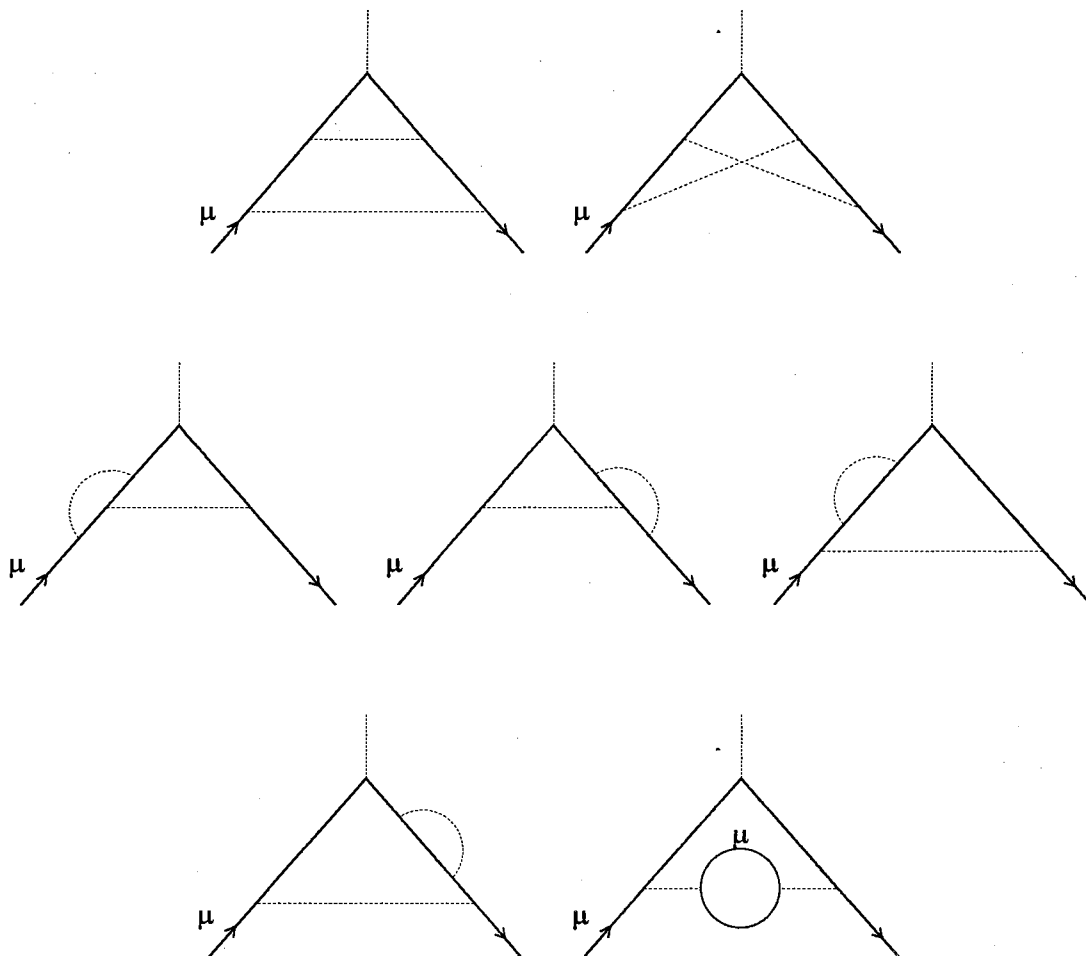


Figure 9. Mass-independent sixth-order vertex diagrams contributing to the muon anomaly

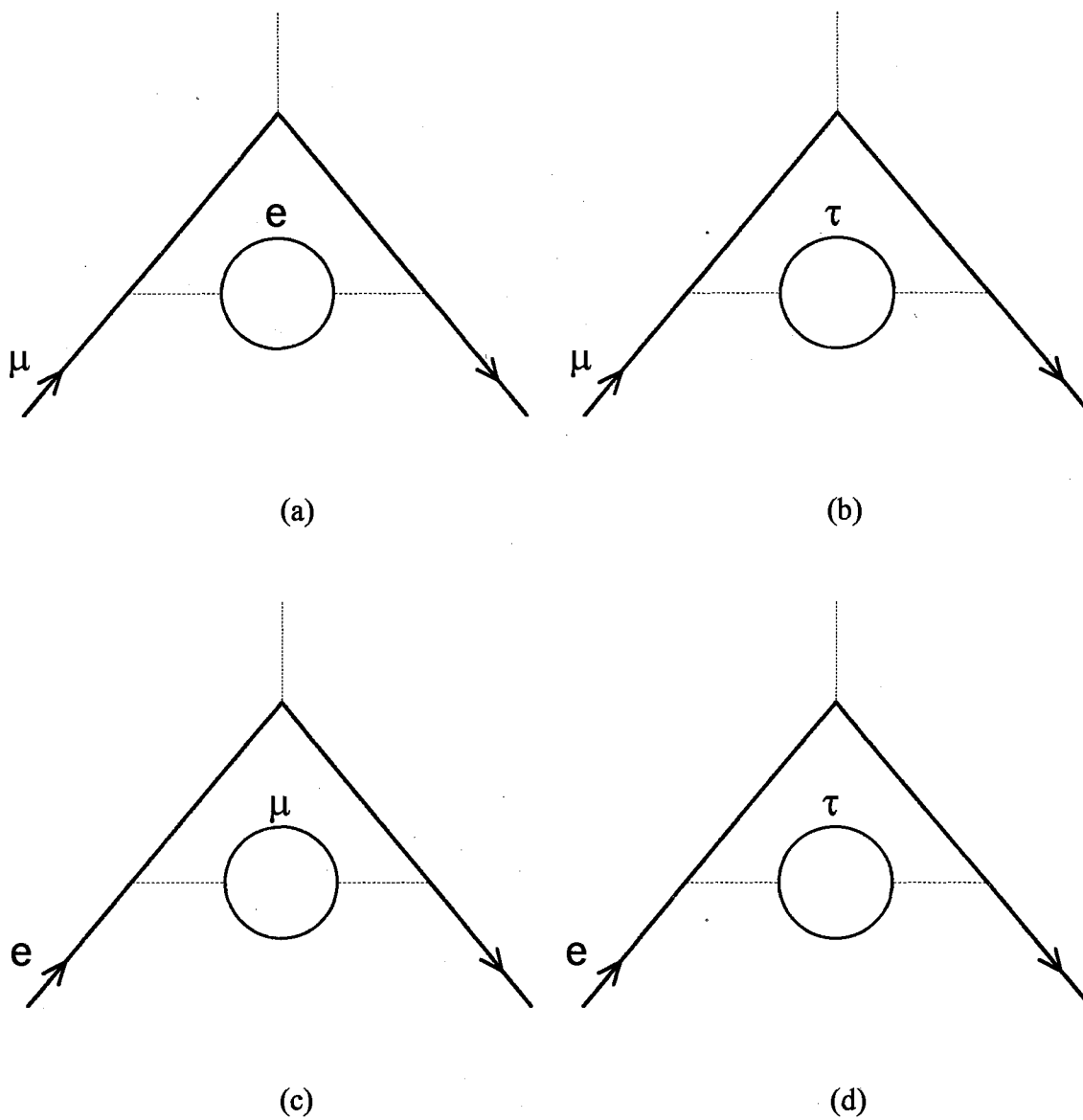


Figure 10. Mass-dependent fourth-order vertex diagrams contributing to the muon anomaly ((a),(b)) and the electron anomaly ((c),(d))

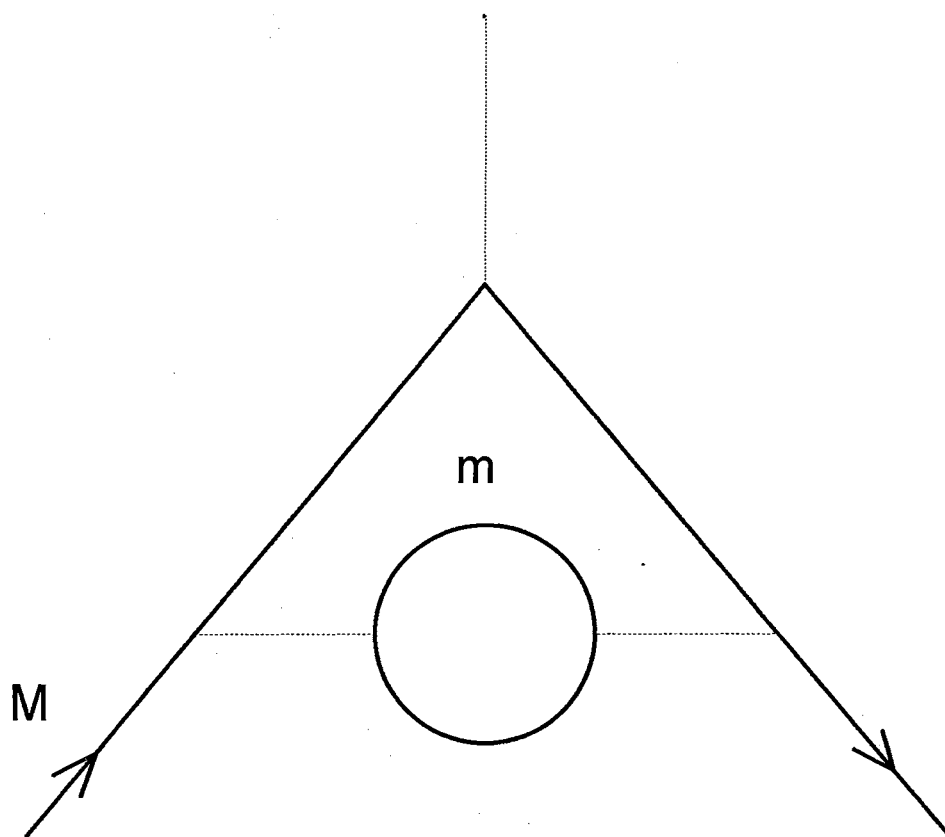


Figure 11. General case of mass-dependent fourth-order vertex diagram

$$f(x) = -\int_0^x dy \frac{\ln|1-y|}{y}. \quad (35)$$

Eq. (34) can be expressed more conveniently in terms of power series of mass ratio $\lambda = m/M$. We have three results corresponding to three cases of λ .

- For $\lambda = k < 1$ we have

$$\begin{aligned} A_2^{(4)} \left[\frac{M}{m} \right] &= -\frac{25}{36} + \frac{\pi^2}{4} k - \frac{1}{3} \ln k + (3 + 4 \ln k) k^2 - \frac{5}{4} \pi^2 k^3 + \left[\frac{\pi^2}{3} + \frac{44}{9} - \frac{14}{3} \ln k + 2 \ln^2 k \right] k^4 \\ &\quad + \frac{8}{15} k^6 \ln k - \frac{109}{225} k^6 + \sum_{n=2}^{\infty} \left[\frac{2(n+3)}{n(2n+1)(2n+3)} \ln k - \frac{8n^3 + 44n^2 + 48n + 9}{n^2(2n+1)^2(2n+3)^2} \right] k^{2n+4}. \end{aligned} \quad (36)$$

- For $\lambda = 1/k > 1$ we get

$$\begin{aligned} A_2^{(4)} \left[\frac{M}{m} \right] &= \frac{k^2}{45} + \frac{k^4 \ln k}{70} + \frac{9}{19600} k^4 - \frac{131}{99225} k^6 + \frac{4k^6}{315} \ln k - \sum_{n=3}^{\infty} \left[\frac{8n^3 + 28n^2 - 45}{[(n+3)(2n+3)(2n+5)]^2} \right] k^{2n+2} \\ &\quad + 2k^2 \ln k \sum_{n=3}^{\infty} \left[\frac{nk^{2n}}{(n+3)(2n+3)(2n+5)} \right]. \end{aligned} \quad (37)$$

- For $\lambda = 1$ we obtain

$$A_2^{(4)} \left[\frac{M}{m} \right] = \frac{119}{36} - \frac{\pi^2}{3}. \quad (38)$$

The major contribution comes from the diagram in Fig. 10(a) which corresponds to $\lambda < 1$ case. From Eq. (36) it easy to find that

$$A_2^{(4)} \left[\frac{m_\mu}{m_e} \right] = 1.09425828(5). \quad (39)$$

The contribution from Figs. 10(b), 10(c), and 10(d) can be obtained from Eq. (37).

For Fig. 10(b) we obtain

$$A_2^{(4)} \left[\frac{m_\mu}{m_\tau} \right] = 7.807(5) \times 10^{-5}. \quad (40)$$

Our result for Fig. 10(c) is

$$A_2^{(4)} \left[\frac{m_e}{m_\mu} \right] = 5.1978(5) \times 10^{-7}, \quad (41)$$

and the contribution due to Fig. 10(d) is negligible:

$$A_2^{(4)} \left[\frac{m_e}{m_\tau} \right] = 2 \times 10^{-9}. \quad (42)$$

The accuracy in Eqs. (39), (40), (41), and (42) is limited only by the experimental accuracy of the measured masses of the charged leptons. When these values are determined more precisely, one can include more terms in the expansions in Eqs. (36) and (37), as needed. Finally we obtain the total fourth order contribution

$$(\alpha_\mu - \alpha_e)^{(4)} = 1.09433583(7) \left[\frac{\alpha}{\pi} \right]^2 = 5904478.4(3) \times 10^{-12}. \quad (43)$$

This differs somewhat with Kinoshita's result

$$(\alpha_\mu - \alpha_e)^{(4)} = 1.0943370 \left[\frac{\alpha}{\pi} \right]^2 = 5904485 \times 10^{-12}. \quad (44)$$

The difference

$$\Delta = \text{ours-Kinoshita's} = -10(1) \times 10^{-12} \quad (45)$$

is due to the fact that we have included more terms in the expansions in Eqs. (36) and (37).

The Sixth-Order Contribution to $(\alpha_\mu - \alpha_e)$

In total, 122 diagrams contribute to $\alpha_\mu^{(6)}$, including 72 mass-independent and 50 mass-dependent diagrams. Again we consider just the mass-dependent diagrams because it is only these diagrams that contribute to $\alpha_\mu - \alpha_e$.

From the previous section we know that the sixth order contribution can be expressed as

$$\begin{aligned}
 (a_\mu - a_e)^{(6)} = & \left\{ A_2^{(6)} \left[\frac{m_\mu}{m_e} \right] + A_2^{(6)} \left[\frac{m_\mu}{m_\tau} \right] + A_3^{(6)} \left[\frac{m_\mu}{m_e}, \frac{m_\mu}{m_\tau} \right] - A_2^{(6)} \left[\frac{m_e}{m_\mu} \right] \right. \\
 & \left. - A_2^{(6)} \left[\frac{m_e}{m_\tau} \right] - A_3^{(6)} \left[\frac{m_e}{m_\mu}, \frac{m_e}{m_\tau} \right] \right\} \left[\frac{\alpha}{\pi} \right]^3.
 \end{aligned} \tag{46}$$

In the following, we will present the analytical and numerical result for each term in Eq. (46) and the corresponding diagrams. $A_2^{(6)}(m_\mu/m_e)$ contains 6 light-by-light scattering diagrams with electron loops (as shown in Fig. 12) and 18 vacuum-polarization diagrams with second and fourth order electron-loop insertions into a fourth order and a sixth order muon vertex, respectively, as shown in Fig. 13.

The light-by-light scattering contribution to $A_2^{(6)}(m_\mu/m_e)$ is known numerically [39]:

$$A_2^{(6)} \left[\frac{m_\mu}{m_e}, \gamma\gamma \right] = 20.9471(20). \tag{47}$$

There is also a new result [40]:

$$A_2^{(6)} \left[\frac{m_\mu}{m_e}, \gamma\gamma \right] = 20.9469(18). \tag{48}$$

It can be seen that there is beautiful agreement between these two results.

The result in Eq. (48) was obtained using VEGAS on our IBM 3090-200S. It required approximately 1500 hours of CPU time and 5×10^{10} function calls. (The integrand used is that of Aldins *et al.* [41].) This result invalidates an earlier result of Samuel and Chlouber [42].

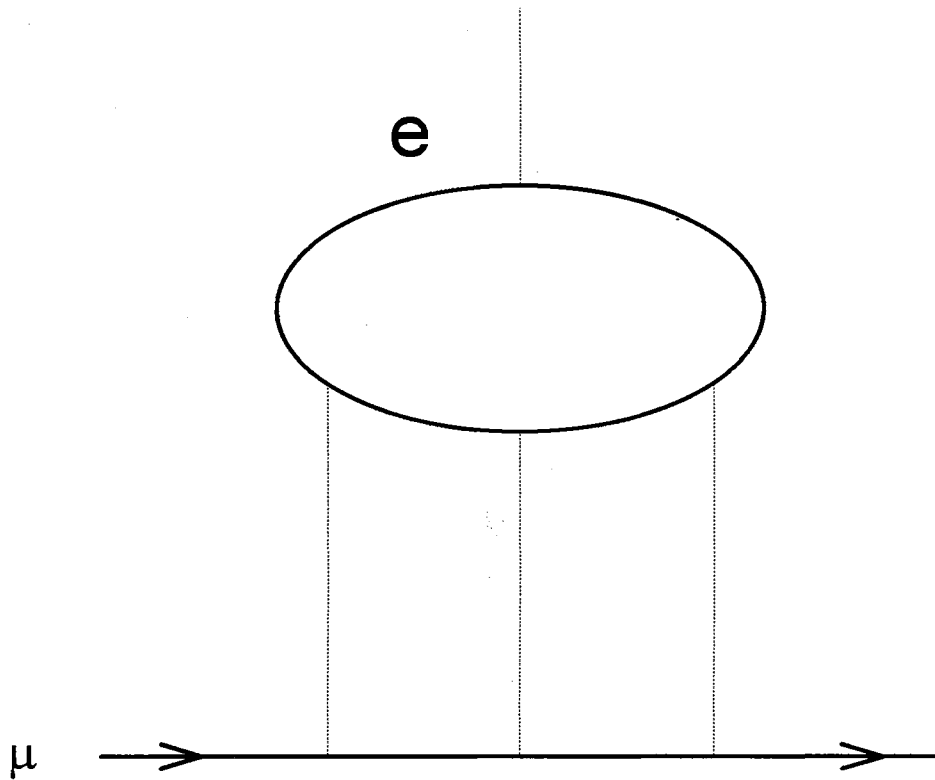


Figure 12. Sixth-order light-by-light scattering diagram contributing to $a_{\mu}^{(6)} - a_e^{(6)}$

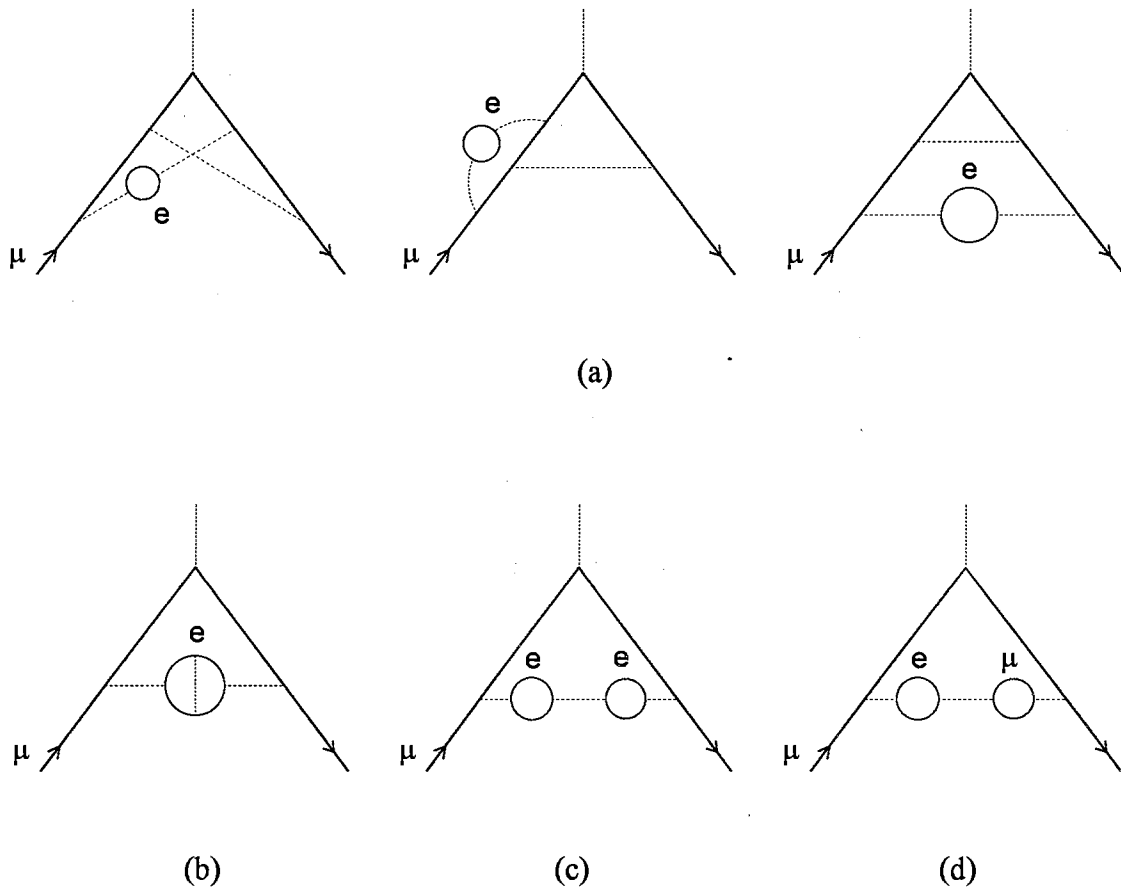


Figure 13. Vacuum-polarization diagrams contributing to $\alpha_\mu^{(6)} - \alpha_e^{(6)}$. (a) second-order-electron-loop-insertion into a fourth-order muon vertex. (b) Proper fourth-order-electron-loop-insertion into a second-order-muon vertex. (c) Double-bubble second-order-electron-loop-insertion into a second-order muon vertex. (d) Mixed-bubble second-order-loop-insertion into a second-order muon vertex.

The vacuum-polarization contributions are calculated separately for each subgroup corresponding to Fig. 13(a), 13(b), 13(c), and 13(d). The contribution from Fig. 13(a) is given by [43]

$$A_2^{(6)}\left[\frac{m_\mu}{m_e}, 13(a)\right] = 2 \int_{4m_e^2}^{\infty} \frac{dt}{t} \cdot \frac{1}{\pi} \text{Im} \pi_e^{(2)}(t) \cdot L_\mu^{(4)}(t), \quad (49)$$

here $\frac{1}{\pi} \text{Im} \pi_e^{(2)}(t)$ is the second-order spectral function

$$\frac{1}{\pi} \text{Im} \pi_e^{(2)}(t) = x \left[\frac{1}{2} - \frac{1}{6} x^2 \right] \cdot \theta(t - 4m_e^2) \quad (50)$$

with

$$x = \sqrt{1 - \frac{4m_e^2}{t}}, \quad (51)$$

and $\theta(t - 4m_e^2)$ is the step function

$$\theta(w) = \begin{cases} 1 & \text{for } w \geq 0 \\ 0 & \text{for } w < 0. \end{cases} \quad (52)$$

For $b \equiv \frac{t}{m_\mu^2} \geq 4$ we have

$$\begin{aligned} L_\mu^{(4)}(t) = & -\frac{31}{16} + \frac{17}{24}b + \left[\frac{1}{4} - \frac{1}{12}b + \frac{7}{16}b^2 + \frac{1}{b-4} \right] \cdot \ln b + \left[\frac{17}{12}b - \frac{49}{24}b^2 + \frac{7}{16}b^3 \right] \\ & \times \frac{\ln y}{\sqrt{b(b-4)}} + \left[\frac{5}{4} - \frac{1}{8}b - \frac{1}{3}b^2 \right] \zeta(2) + \frac{5}{96}b^2 \ln^2 b + \left[-\frac{1}{2}b + \frac{17}{24}b^2 \right. \\ & \left. - \frac{7}{48}b^3 \right] \cdot \frac{\ln b \cdot \ln y}{\sqrt{b(b-4)}} + \left[\frac{7}{24} + \frac{15}{16}b - \frac{7}{32}b^2 + \frac{2}{b-4} \right] \cdot \ln^2 y \\ & + \left[-2b + \frac{17}{6}b^2 - \frac{7}{12}b^3 \right] \cdot \frac{D_p(b)}{\sqrt{b(b-4)}} + \left[-1 + \frac{b}{6} + \frac{19}{12}b^2 - \frac{b^3}{2} - \frac{4}{b-4} \right] \\ & \times \frac{D_m(b)}{\sqrt{b(b-4)}} + \left[\frac{1}{2} - \frac{7}{6}b + \frac{1}{2}b^2 \right] \cdot T(b) \end{aligned} \quad (53)$$

with

$$y = \frac{\sqrt{b} - \sqrt{b-4}}{\sqrt{b} + \sqrt{b-4}}, \quad (54)$$

$$D_p(b) = Li_2(y) + \ln y \cdot \ln(1-y) - \frac{1}{4} \ln^2 y - \zeta(2), \quad (55)$$

$$D_m(b) = Li_2(-y) + \frac{1}{4} \ln^2 y + \frac{1}{2} \zeta(2), \quad (56)$$

and

$$\begin{aligned} T(b) = & -6Li_3(y) - 3Li_3(-y) + \ln^2 y \cdot \ln(1-y) \\ & + \frac{1}{2} [\ln^2 y + 6\zeta(2)] \cdot \ln(1+y) + 2[Li_2(-y) + 2Li_2(y)] \cdot \ln y, \end{aligned} \quad (57)$$

where the functions $Li_2(y)$ and $Li_3(y)$ are the dilogarithm and trilogarithm defined through

$$Li_2(y) = -\int_0^y \frac{dt}{t} \ln(1-t), \quad Li_3(y) = \int_0^y \frac{dt}{t} Li_2(y). \quad (58)$$

After a very tedious calculation we get

$$\begin{aligned} A_2^{(6)} \left[\frac{m_\mu}{m_e}, 13(a) \right] = & \left[-\frac{31}{12} + \frac{5}{9} \pi^2 - \frac{2}{3} \pi^2 \ln 2 + \zeta(3) \right] \ln \left[\frac{m_\mu}{m_e} \right] + \frac{115}{24} - \frac{79}{54} \pi^2 \\ & + \frac{5}{3} \pi^2 \ln 2 - \frac{7}{2} \zeta(3) + 3c_4 + \frac{\pi^2}{8} \left[\frac{m_e}{m_\mu} \right] - 4 \left[\frac{m_e}{m_\mu} \right]^2 \ln \left[\frac{m_\mu}{m_e} \right] \\ & + \left[\frac{111}{36} \pi^2 + 7\zeta(3) - \frac{315}{54} - \frac{14\pi^2}{3} \ln 2 \right] \left[\frac{m_e}{m_\mu} \right]^2 \\ & + O \left[\left[\frac{m_e}{m_\mu} \right]^3 \ln \left[\frac{m_\mu}{m_e} \right] \right] \\ = & -2.392396(6) + O \left[\left[\frac{m_e}{m_\mu} \right]^3 \ln \left[\frac{m_\mu}{m_e} \right] \right]. \end{aligned} \quad (59)$$

The contribution from Fig. 13(b) is given by [44]

$$A_2^{(6)} \left[\frac{m_\mu}{m_e}, 13(b) \right] = \int_{4m_e^2}^{\infty} \frac{dt}{t} \cdot \frac{1}{\pi} \text{Im} \pi_e^{*(4)}(t) K_\mu^{(2)}(t), \quad (60)$$

where

$$\begin{aligned} \frac{1}{\pi} \text{Im} \pi_{e^*}^{*(4)}(t) = & \left\{ x \left[\frac{5}{8} - \frac{3}{8} x^2 + \left(-\frac{1}{2} + \frac{1}{6} x^2 \right) \cdot \ln \frac{64x^2}{(1-x^2)^3} \right] + \left[\frac{11}{16} + \frac{11}{24} x^2 \right. \right. \\ & \left. \left. - \frac{7}{48} x^4 + \left(\frac{1}{2} + \frac{1}{3} x^2 - \frac{1}{6} x^4 \right) \cdot \ln \frac{(1+x)^3}{8x^2} \right] \cdot \ln \frac{1+x}{1-x} \right. \\ & \left. - \left[\frac{1}{2} + \frac{1}{3} x^2 - \frac{1}{6} x^4 \right] \cdot \left[4\Phi \left(-\frac{1-x}{1+x} \right) + 2\Phi \left(\frac{1-x}{1+x} \right) + \frac{1}{2} \pi \right] \right\} \\ & \times \theta(t - 4m_e^2) \end{aligned} \quad (61)$$

$$\Phi(z) = \int_1^z du \frac{\ln(1+u)}{u}, \quad (62)$$

and

$$K_\mu^{(2)}(t) = \int_0^1 dz \frac{z^2(1-z)}{z^2 + (t/m_\mu^2)(1-z)} \quad (63)$$

is the second-order contribution from the exchange of a photon with squared mass t . The explicit form of $K_\mu^{(2)}(t)$ is the following [45]:

- for $0 \leq t \leq 4m_\mu^2$, with $u = t/4m_\mu^2$

$$K_\mu^{(2)}(t) = \left[\frac{1}{2} - 4u - 4u(1-2u) \ln(4u) - 2(1-8u+8u^2) \sqrt{\frac{u}{1-u}} \arccos \sqrt{u} \right], \quad (64)$$

- for $t \geq 4m_\mu^2$, with $v = \frac{1 - \sqrt{1 - 4m_\mu^2/t}}{1 + \sqrt{1 - 4m_\mu^2/t}}$

$$K_\mu^{(2)}(t) = \frac{1}{2} v^2 (2 - v^2) + (1+v)^2 (1+v^2) \frac{\ln(1+v) - v + \frac{1}{2} v^2}{v^2} + \frac{1+v}{1-v} v^2 \ln v. \quad (65)$$

The result turns out to be

$$A_2^{(6)} \left[\frac{m_\mu}{m_e}, 13(b) \right] = \frac{1}{4} \ln \left[\frac{m_\mu}{m_e} \right] + \frac{1}{2} \zeta(3) - \frac{5}{12} + \left[-\frac{13}{18} \pi^3 - \frac{16}{9} \pi^2 \ln 2 \right]$$

$$\begin{aligned}
& + \frac{79}{27} \pi^2 \left[\frac{m_e}{m_\mu} \right] + 6 \left[\frac{m_e}{m_\mu} \right]^2 \ln^2 \left[\frac{m_\mu}{m_e} \right] - 3 \left[\frac{m_e}{m_\mu} \right]^2 \ln \left[\frac{m_\mu}{m_e} \right] \\
& + \left[\pi^2 + \frac{35}{3} - 9\zeta(3) \right] \left[\frac{m_e}{m_\mu} \right]^2 + O \left[\left[\frac{m_e}{m_\mu} \right]^3 \ln^2 \left[\frac{m_\mu}{m_e} \right] \right] \\
& = 1.49367(3) + O \left[\left[\frac{m_e}{m_\mu} \right]^3 \ln^2 \left[\frac{m_\mu}{m_e} \right] \right].
\end{aligned} \tag{66}$$

The contribution due to Fig. 13(c) is given by [46]

$$A_2^{(6)} \left[\frac{m_\mu}{m_e}, 13(c) \right] = \int_{4m_e^2}^{\infty} \frac{dt}{t} \text{Im} \pi_e^{(4)}(t) K_\mu^{(2)}(t), \tag{67}$$

where $K_\mu^{(2)}(t)$ is given by Eq. (63) and

$$\text{Im} \pi_e^{(4)}(t) = -2 \text{Re} \pi_e^{(2)}(t) \tag{68}$$

with

$$\frac{1}{\pi} \text{Re} \pi_e^{(2)}(t) = \left[\frac{8}{9} - \frac{1}{3} x^2 + \left(\frac{1}{2} - \frac{1}{6} x^2 \right) x \ln \frac{1-x}{1+x} \right], \tag{69}$$

and the definition of x is given by Eq. (51).

The final result is

$$\begin{aligned}
A_2^{(6)} \left[\frac{m_\mu}{m_e}, 13(c) \right] &= \frac{2}{9} \ln^2 \left[\frac{m_\mu}{m_e} \right] - \frac{25}{27} \ln \left[\frac{m_\mu}{m_e} \right] + \frac{317}{324} + \frac{\pi^2}{27} - \frac{4\pi^2}{45} \left[\frac{m_e}{m_\mu} \right] \\
& - \frac{8}{3} \left[\frac{m_e}{m_\mu} \right]^2 \ln^2 \left[\frac{m_\mu}{m_e} \right] + \frac{52}{9} \left[\frac{m_e}{m_\mu} \right]^2 \ln \left[\frac{m_\mu}{m_e} \right] \\
& - \left[\frac{4}{9} \pi^2 + 4 \right] \left[\frac{m_e}{m_\mu} \right]^2 + O \left[\left[\frac{m_e}{m_\mu} \right]^3 \ln^2 \left[\frac{m_\mu}{m_e} \right] \right] \\
& = 2.71866(3) + O \left[\left[\frac{m_e}{m_\mu} \right]^3 \ln^2 \left[\frac{m_\mu}{m_e} \right] \right].
\end{aligned} \tag{70}$$

For Fig. 13(d), the contribution is given by [43]

$$A_2^{(6)}\left[\frac{m_\mu}{m_e}, 13(d)\right] = 2 \int_{4m_e^2}^{\infty} \frac{dt}{t} \cdot \frac{1}{\pi} \text{Im} \pi_e^{(2)}(t) \cdot M_\mu^{(4)}(t), \quad (71)$$

where

$$\begin{aligned} M_\mu^{(4)}(t) = & \frac{35}{36} + \frac{8}{9}b + \left[\frac{4}{3} - \frac{1}{9}b - \frac{5}{18}b^2\right] \cdot \ln b + \left[-\frac{4}{3} + \frac{19}{9}b + \frac{4}{9}b^2 - \frac{5}{18}b^3\right] \\ & \times \frac{\ln y}{\sqrt{b(b-4)}} + \left[1 + \frac{1}{3}b - \frac{1}{6}b^2 - \frac{2}{b}\right] \zeta(2) \\ & + \left[\frac{1}{2} + \frac{1}{6}b - \frac{1}{12}b^2 - \frac{1}{3b}\right] \cdot \ln^2 y + \left[\frac{16}{3} - \frac{4b}{3} - \frac{4}{3}b^2 + \frac{b^3}{3}\right] \times \frac{D_m(b)}{\sqrt{b(b-4)}}, \end{aligned} \quad (72)$$

and the definitions of b and $D_m(b)$ are the same as those in Eq. (53).

The complicated calculation gives

$$\begin{aligned} A_2^{(6)}\left[\frac{m_\mu}{m_e}, 13(d)\right] = & \left[\frac{119}{27} - \frac{4}{9}\pi^2\right] \ln\left[\frac{m_\mu}{m_e}\right] - \frac{61}{162} + \frac{\pi^2}{27} + \left[\frac{4\pi^2}{9} - \frac{115}{27}\right] \left[\frac{m_e}{m_\mu}\right]^2 \\ & + O\left[\left[\frac{m_e}{m_\mu}\right]^3\right] \\ = & 0.100519(1) + O\left[\left[\frac{m_e}{m_\mu}\right]^3\right], \end{aligned} \quad (73)$$

where

$$c_4 = \frac{11}{648}\pi^4 - \frac{2}{27}\pi^2 \ln^2 2 - \frac{1}{27}\ln^4 2 - \frac{8}{9}a_4, \quad (74)$$

$$a_4 = \sum_{n=1}^{\infty} \frac{1}{2^n n^4} = 0.517479061, \quad (75)$$

and

$$\zeta(3) = \sum_{n=1}^{\infty} \frac{1}{n^3} = 1.202056903. \quad (76)$$

Our errors are estimated by multiplying the next uncalculated term by ten. Our results in Eqs. (59), (66), (70) and (73) agree with the previously known results to $O(m_e/m_\mu)$ given in Refs. [46,47,48,49], respectively.

The presence of the $(m_e/m_\mu)^2 \ln^2(m_\mu/m_e)$ terms in Eqs. (66) and (70) are somewhat surprising.

The total vacuum-polarization contribution in sixth order is

$$A_2^{(6)} \left[\frac{m_\mu}{m_e}, \text{vp} \right] = 1.92045(5). \quad (77)$$

After multiplying by $(\alpha/\pi)^3$, we obtain our result

$$(\alpha_\mu^{(6)} - \alpha_e^{(6)})(\text{vp}) = 24068.5(6) \times 10^{-12}. \quad (78)$$

These results in Eqs. (59), (66), (70), and (73) should be compared with Kinoshita's new results given in Table I [50]. His total sixth-order vacuum polarization result to be compared with Eq. (78) is

$$(\alpha_\mu^{(6)} - \alpha_e^{(6)})(\text{vp}, \text{K}) = 24069(6) \times 10^{-12}. \quad (79)$$

The agreement is excellent!

Adding Eqs. (47) and (77), we get the sixth order result

$$A_2^{(6)} \left[\frac{m_\mu}{m_e} \right] = 22.8674(18). \quad (80)$$

Next, we consider the contribution from $A_2^{(6)}(m_\mu/m_\tau)$. The corresponding diagrams can be obtained by replacing the electron in those graphs for $A_2^{(6)}(m_\mu/m_e)$ by the τ . However, the results cannot be simply obtained in this way, due to the difference in the masses of the electron and the tau.

As in the case of $A_2^{(6)}(m_\mu/m_e)$, we again divide $A_2^{(6)}(m_\mu/m_\tau)$ into two parts: light-by-light scattering and vacuum-polarization subgraphs. They are represented by

TABLE I

COMPARISON OF $A_2^{(6)}(m_\mu/m_e, \nu p)$ WITH KINOSHITA'S
RESULTS. SEE APPENDIX A-2

Figure	Ours	Kinoshita	$\Delta(\alpha/\pi)^3 (10^{-12})$	$\Delta'(\alpha/\pi)^3 (10^{-12})$
13(a)	-2.392396(6)	-2.39238(43)	0(5)	-69(5)
13(b)	1.49367(3)	1.49373(13)	-1(2)	295(2)
13(c)	2.71866(3)	2.71863(5)	0(1)	69(1)
13(d)	0.100519(1)	0.100519(5)	0	0
Total	1.92045(5)	1.92050(45)	-1(6)	295(5)

$A_2^{(6)}(m_\mu/m_\tau, \gamma\gamma)$ and $A_2^{(6)}(m_\mu/m_\tau, \nu\bar{\nu})$, respectively. We can estimate $A_2^{(6)}(m_\mu/m_\tau, \gamma\gamma)$ by using Aldins *et al* [51]. Our result is (Fig. 12 with $e \rightarrow \tau$)

$$A_2^{(6)}\left[\frac{m_\mu}{m_\tau}, \gamma\gamma\right] = 1.836 \times 10^{-3}. \quad (81)$$

As for $A_2^{(6)}(m_\mu/m_\tau, \nu\bar{\nu})$, we have analytical expressions for all the diagrams. These formulas were derived by Barbieri and Remiddi [43] in calculating the muon contribution to the electron anomaly and can be applied to our cases. The results corresponding to Fig. 14 and 15 are given by, respectively,

$$\begin{aligned} A_2^{(6)}\left[\frac{m_\mu}{m_e}, \text{Fig. 14}\right] &= -\frac{2}{3}\left[\frac{m_\mu}{m_\tau}\right]^2 \left[-\frac{2689}{5400} + \frac{\pi^2}{15} + \frac{23}{90} \ln \frac{m_\tau}{m_\mu} \right] \\ &= -2.063 \times 10^{-3}, \end{aligned} \quad (82)$$

$$A_2^{(6)}\left[\frac{m_\mu}{m_\tau}, \text{Fig. 15}\right] = \frac{41}{486}\left[\frac{m_\mu}{m_\tau}\right]^2 = 0.296 \times 10^{-3}. \quad (83)$$

Combining all the contributions in Eqs.(81), (82), and (83), we obtain the total value for $A_2^{(6)}(m_\mu/m_\tau)$:

$$A_2^{(6)}\left[\frac{m_\mu}{m_\tau}\right] = 6.9 \times 10^{-5}. \quad (84)$$

We see that a large cancellation makes the total contribution from the τ nearly negligible.

Now we come to the term $A_3^{(6)}(m_\mu/m_e, m_\mu/m_\tau)$. There are two diagrams corresponding to this contribution, as shown in Fig. 16. Generally for a two-bubble diagram shown in Fig. 17, we have the expression

$$A_3^{(6)}\left[\frac{m}{m_1}, \frac{m}{m_2}\right] = \int_0^1 dx (1-x) [-\pi(x, k_1)] [-\pi(x, k_2)], \quad (85)$$

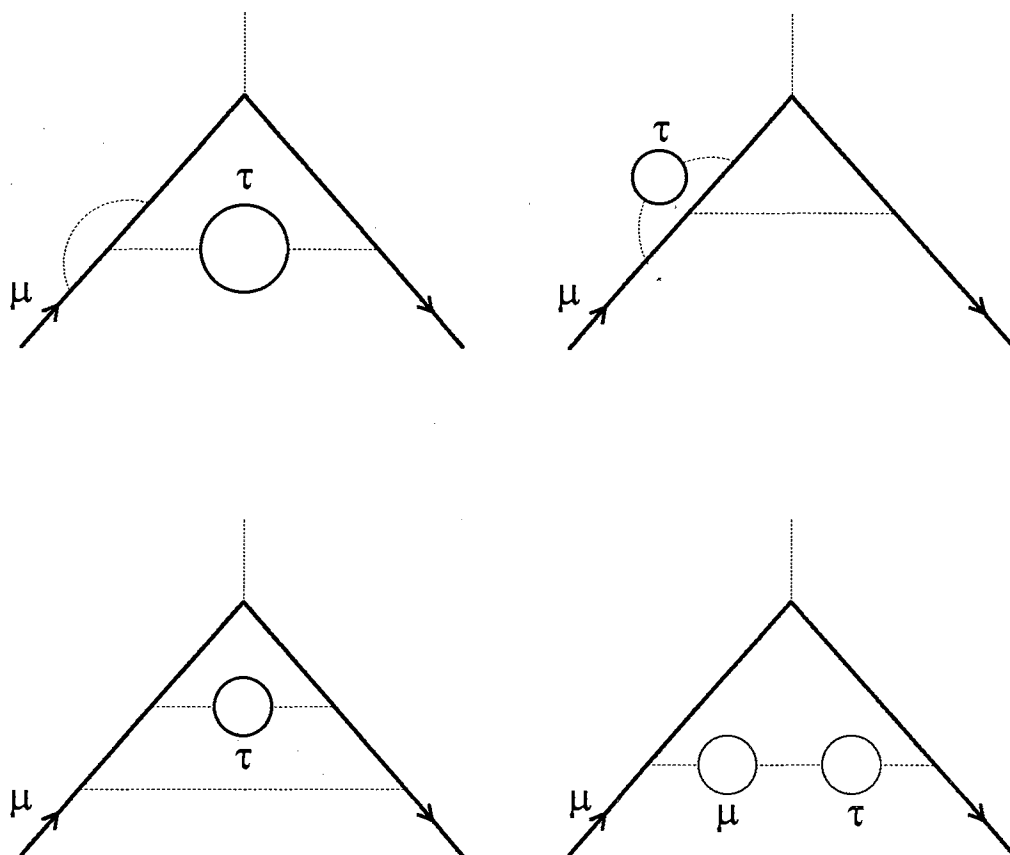


Figure 14. Second-order τ -loop-insertion into a fourth-order muon vertex.

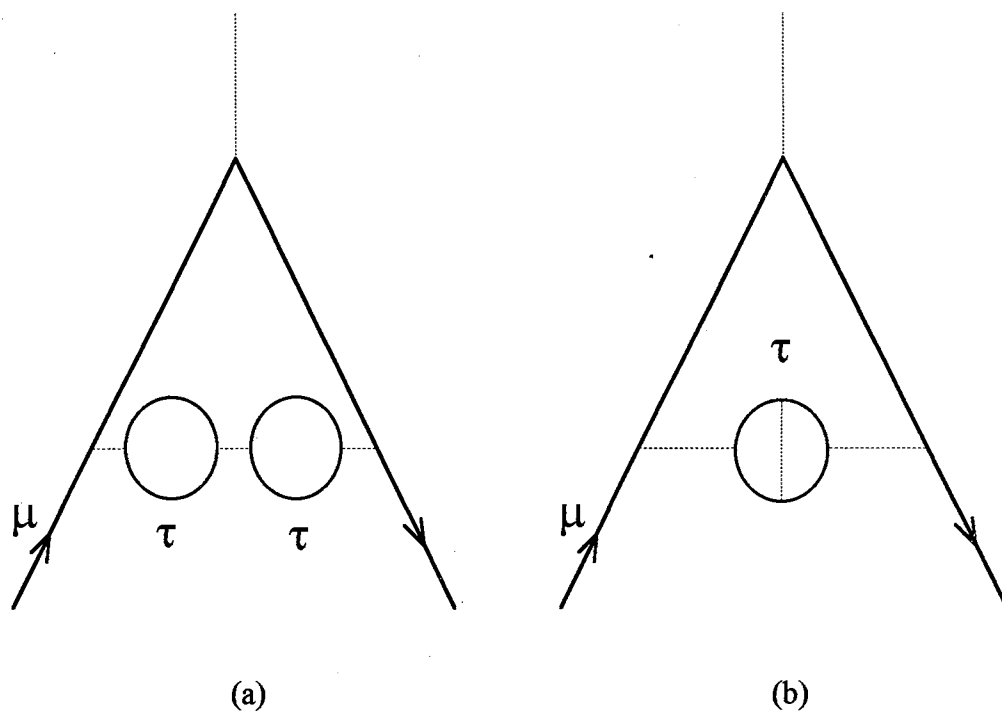


Figure 15. Fourth-order τ -loop-insertion into a second-order muon vertex.

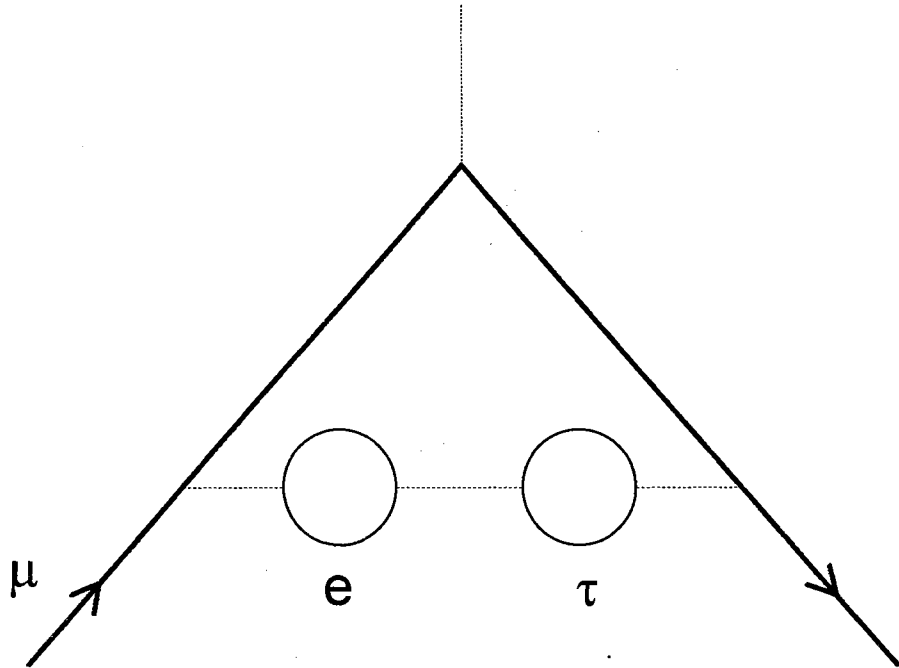


Figure 16. Sixth-order mixed bubble vertex diagram contributing to the muon anomaly

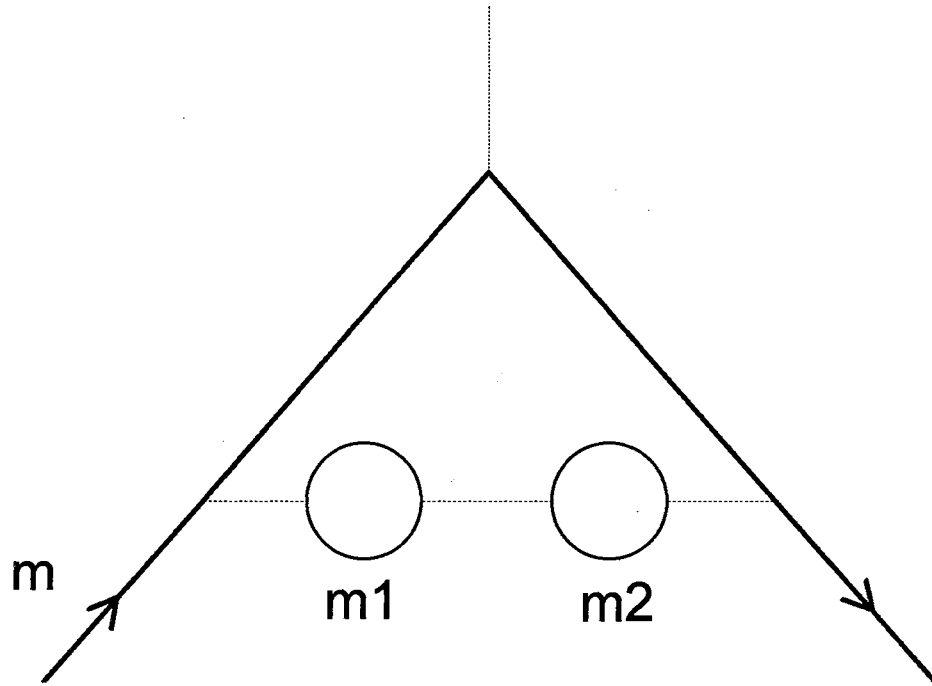


Figure 17. General case of mass-dependent sixth-order vertex diagram

where

$$\pi(x, k_p) = \frac{8}{9} - \frac{B_p^2}{3} + \left[\frac{1}{2} - \frac{B_p^2}{6} \right] B_p \ln \left[\frac{B_p - 1}{B_p + 1} \right], \quad (86)$$

and

$$B_p(x) = \left[1 + \frac{4(1-x)}{x^2} k_p^2 \right]^{1/2}, \quad k_p = \frac{m_p}{m} \quad (p = 1, 2). \quad (87)$$

In principle, one can find an analytical expression for $A_3^{(6)}(m/m_1, m/m_2)$. But a numerical result is sufficient. We have

$$A_3^{(6)} \left[\frac{m_\mu}{m_e}, \frac{m_\mu}{m_\tau} \right] = 5.24 \times 10^{-4}. \quad (88)$$

This result agrees with Kinoshita's result to three significant figures.

Other contributions to $\alpha_\mu^{(6)} - \alpha_e^{(6)}$ come from the anomalous magnetic moment of the electron. That is, $A_2^{(6)}(m_e/m_\mu)$, $A_2^{(6)}(m_e/m_\tau)$ and $A_3^{(6)}(m_e/m_\mu, m_e/m_\tau)$. The corresponding diagrams can be obtained by exchanging the electron and the muon in Fig.12,13,15, and 16 and by replacing the muon by the electron in Fig. 14. One can use the method used in calculating $A_2^{(6)}(m_\mu/m_e)$, $A_2^{(6)}(m_\mu/m_\tau)$ and $A_3^{(6)}(m_\mu/m_e, m_\mu/m_\tau)$ to compute these contributions. However these terms are very small and can be neglected.

Now we are in a position to get the total contribution in sixth order. Adding up Eqs. (80), (84), and (88) we have

$$(\alpha_\mu - \alpha_e)^{(6)} = 22.8677(18) \left[\frac{\alpha}{\pi} \right]^3. \quad (89)$$

The QED Contribution up to Tenth-Order

In the previous two sections, we calculated the fourth order and sixth order contributions to $(a_\mu - a_e)$. The contribution in eighth order that dominated is the contribution of the class of diagrams obtained by inserting an electron bubble in a leg of Fig. 12. Our 1977 result [52] is

$$a_\mu^{(8)}(\gamma\gamma) = 117.4(5). \quad (90)$$

This agrees with Kinoshita's recent result [5,6]

$$a_\mu^{(8)}(\gamma\gamma) = 116.8(1). \quad (91)$$

By using Kinoshita's total contributions for the eighth and tenth order,

$$(a_\mu - a_e)^{(8)} = 127.00(41) \left[\frac{\alpha}{\pi} \right]^4, \quad (92)$$

$$(a_\mu - a_e)^{(10)} = 570(140) \left[\frac{\alpha}{\pi} \right]^5, \quad (93)$$

we can obtain the total QED contribution which is given by

$$\begin{aligned} (a_\mu - a_e)^{\text{QED}} &= 1.09433583(7) \left[\frac{\alpha}{\pi} \right]^2 + 22.8680(18) \left[\frac{\alpha}{\pi} \right]^3 + 127.00(41) \left[\frac{\alpha}{\pi} \right]^4 \\ &\quad + 570(140) \left[\frac{\alpha}{\pi} \right]^5 \\ &= 6194812(27) \times 10^{-12}. \end{aligned} \quad (94)$$

Adding the anomalous magnetic moment a_e , given by Eq. (26), to Eq. (94), and subtracting

$$a_e^{\text{hadronic}} + a_e^{\text{weak}} = 1.6 \times 10^{-12}, \quad (95)$$

we can find the pure QED contribution to the muon anomaly which is

$$a_\mu^{\text{QED}} = 1165846950(28)(27) \times 10^{-12}. \quad (96)$$

where the first error comes from the uncertainty in α and the second one comes from the sixth, eighth and tenth order contributions.

This should be compared to Kinoshita's value

$$a_{\mu}^{\text{QED}}(\text{K}) = 1165846961(44)(27) \times 10^{-12}, \quad (97)$$

the first error is an estimate of the theoretical uncertainty and the second reflects the uncertainty in α . Thus the difference is

$$\begin{aligned} a_{\mu}^{\text{QED}} - a_{\mu}^{\text{QED}}(\text{K}) &= (-7 - 1 - 2 + 1 - 3) \times 10^{-12} \\ &= -12 \times 10^{-12}. \end{aligned} \quad (98)$$

This difference reflects the uncertainty coming from the uncalculated terms in our analytical calculations and the uncertainty in the numerical integrations in Kinoshita's results where the -7 comes from fourth-order, the -1 comes from sixth-order, the -2 comes from a_e^{hadronic} , the 1 comes from the τ contribution and the -3 from the light-by-light contribution.

Non-QED Contributions and the Muon Anomaly

Unlike the anomalous magnetic moment of the electron, which is dominated by the QED effect due to the smallness of its mass, the anomaly of the muon has substantial contributions from hadronic and weak interactions. Unfortunately, those contributions have not yet been computed very accurately. So far the best estimates are [52,53,54]

$$a_{\mu}^{\text{hadronic}} = 7011(76) \times 10^{-11}, \quad (99)$$

$$a_{\mu}^{\text{weak}} = 195(10) \times 10^{-11}, \quad (100)$$

where the hadronic contribution includes fourth and sixth order and the weak contribution includes only the one-loop contribution [55].

Although we use the result of Ref. [54] for a_μ^{hadronic} , it should be noted that the error in Eq. (99) may be overly optimistic. More accurate experiments to measure $\sigma(e^+e^- \rightarrow \text{hadrons})$ are urgently needed to reduce the error in Eq. (99).

Collecting all the contributions from QED, hadronic, and weak effects, we finally find the anomaly of the muon

$$a_\mu^{\text{theory}} = 116591902(77) \times 10^{-11}, \quad (101)$$

which is in very good agreement with the experimental value

$$a_\mu^{\text{expt}} = 1165923(8.5) \times 10^{-9} \quad (7 \text{ ppm}). \quad (102)$$

Equations (101) and (102) should be compared to Kinoshita's value

$$a_\mu^{\text{theory}} = 116591919(176) \times 10^{-11}. \quad (103)$$

Our result given in Eq. (101) implies the following value for the gyromagnetic ratio g_μ :

$$g_\mu = 2.00233183804(154). \quad (104)$$

Kinoshita's result in Eq. (103) implies

$$g_\mu = 2.00233183838(352). \quad (105)$$

These results in Eqs.(104) and (105) should be compared with the present experimental value

$$g_\mu = 2.002331846(17). \quad (106)$$

Recently Laporta and Remiddi have obtained a more accurate result for the contribution from the light-by-light diagram in the sixth order [56]. Their result is

$$A_2^{(6)}(m_\mu/m_e, \gamma\gamma) = 20.9479242(9). \quad (107)$$

If we use this new value, we can get the following results:

$$(a_\mu - a_e)^{\text{QED}} = 6194828(27) \times 10^{-12}, \quad (108)$$

$$\alpha_\mu^{\text{QED}} = 1165846966(28)(27) \times 10^{-12}, \quad (109)$$

$$\alpha_\mu^{\text{theory}} = 116591904(77) \times 10^{-11}, \quad (110)$$

and

$$g_\mu = 2.00233183808(154). \quad (111)$$

In the Appendix A, we will give a detailed comparison between our results and Kinoshita's results.

CHAPTER IV

ANOMALOUS MAGNETIC MOMENT OF THE TAU

The τ lepton was discovered in 1975 [57]. All evidence indicates that it is a SM lepton [58]. A very important property of the τ , which has yet to be calculated, is its magnetic moment,

$$\mu_\tau = \frac{g_\tau e\hbar}{2m_\tau c} \quad (112)$$

given by its anomaly

$$a_\tau = \frac{g_\tau - 2}{2}. \quad (113)$$

Although g_μ has not yet been measured, it may be possible in the future, in spite of the obvious difficulty involved in such an experiment. This could be done by making use of the radiation amplitude zero [59] which occurs at the high-energy end of the lepton distribution in radiative τ decays. This zero amplitude will be noticeable only if $g_\tau \approx 2$. Of course, very good energy resolution would be necessary. A measurement of the anomalous magnetic moment of the τ lepton using this method has been suggested by Perl [60]. This could be done at a proposed Tau-Charm Factory, where approximately 10^8 τ pairs would be produced, via the reaction $e^+e^- \rightarrow \tau^+\tau^-$ at a c.m. energy of 3.67 Gev. or at the recently approved B Factory at SLAC. An alternative method would be to make use of channeling [61] in a bent crystal, which has been suggested for measuring baryon magnetic moments, where the baryon has a short lifetime, $\tau \approx 10^{-13}$ s. [The lifetime of the τ is $\tau = 0.303(8) \times 10^{-12}$ s.] The strong electric field is seen by the fast-moving particle as a large megatesla magnetic field and the spin will precess significantly

before it decays. This can be measured from the angular distribution of its decay lepton. From the precession angle one can obtain g . Such an experiment, to test the method, has been done at Fermilab (E761). The decay $\Sigma^+ \rightarrow p\gamma$ was being used to measure the magnetic moment of the Σ^+ , μ_{Σ^+} . The crystal used was Si. Preliminary results indicate that the method works and an accurate value for μ_{Σ^+} was obtained [62]. This is a fixed-target experiment. For the τ one could use the decay $B^+ \rightarrow \tau^+ \nu$, which would produce polarized τ leptons. The spin would then precess in a bent crystal and could be measured from the angular distribution of the $\mu(e)$ in the leptonic decay of the τ , $\tau \rightarrow \mu(e) \nu \bar{\nu}$. Such an experiment might be possible at the Tevatron at Fermilab or at the Large Hadron Collider (LHC), if fixed-target experiments will be possible there. We hope that this option will be seriously considered. However, independent of the experimental situation we believe a prediction for the magnetic moment of the τ lepton is important from a purely theoretical point of view.

In calculating the anomalous magnetic moment of τ , we follow the procedure used in the case of the muon by first calculating the mass-dependent contribution to $a_\tau - a_e$, and then in the end using the known value for a_e :

$$a_\tau = (a_\tau - a_e) + a_e. \quad (114)$$

In our case the τ receives contributions from the electron and the muon:

$$a_\tau - a_e = A \left[\frac{m_\tau}{m_e} \right] + A \left[\frac{m_\tau}{m_\mu} \right] + A \left[\frac{m_\tau}{m_e}, \frac{m_\tau}{m_\mu} \right], \quad (115)$$

where the third term, which depends on all three leptons, occurs only in sixth and higher orders. The mass-dependent contributions for a_e are negligible.

In fourth order the contributions from Figs. 18(a) and 18(b) are given by Eq. (39) with $k = m_e/m_\tau$, and $k = m_\mu/m_\tau$, respectively. The results are

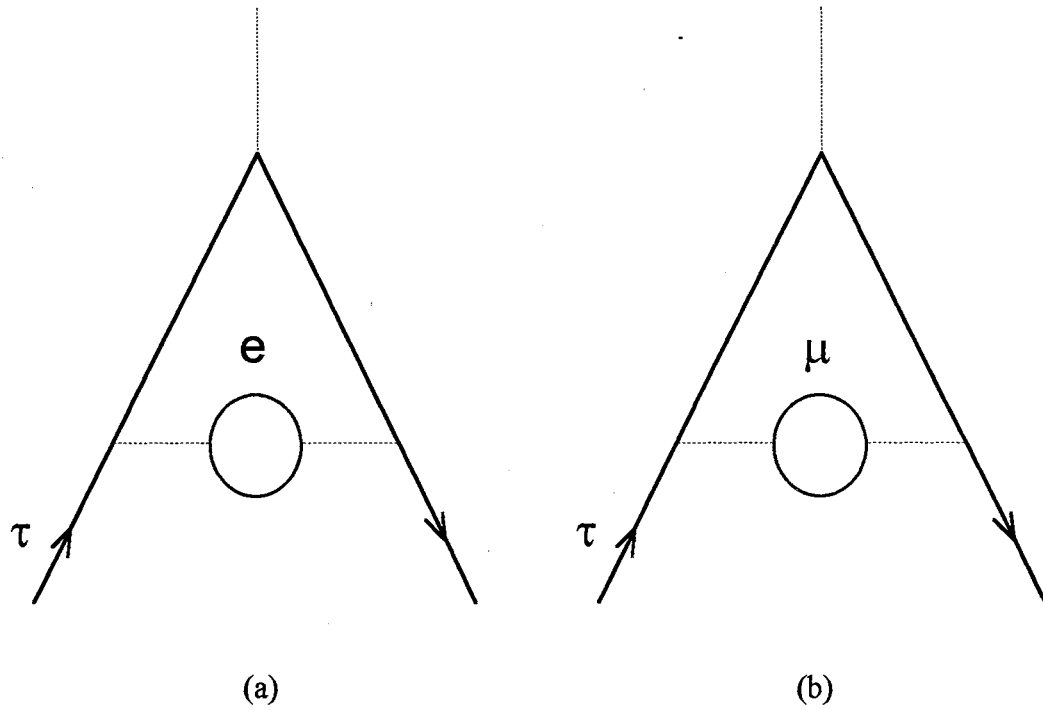


Figure 18. Mass-dependent fourth-order vertex diagram contributing to the tau anomaly

$$A_2^{(4)} \left[\frac{m_\tau}{m_e} \right] = 2.0243(1) \left[\frac{\alpha}{\pi} \right]^2 = 1.09221(5) \times 10^{-5}, \quad (116)$$

and

$$A_2^{(4)} \left[\frac{m_\tau}{m_\mu} \right] = 0.36164(7) \left[\frac{\alpha}{\pi} \right]^2 = 0.19512(4) \times 10^{-5}. \quad (117)$$

Thus the total contribution in fourth order is given by

$$(a_\tau - a_e)^{(4)} = 1.28733(6) \times 10^{-5}. \quad (118)$$

In the sixth order the dominant contribution comes from the light-by-light scattering diagrams illustrated in Fig. 19. The contribution of Fig. 19(a) is given by

$$A_2^{(6)} \left[\frac{m_\tau}{m_e}, \gamma\gamma \right] = \left[\frac{2\pi^2}{3} \ln \frac{m_\tau}{m_e} + B \right] \left[\frac{\alpha}{\pi} \right]^3, \quad (119)$$

where B can be obtained from two independent calculations [40,39], which agree to the accuracy needed here:

$$B = -14.13. \quad (120)$$

Thus we obtain

$$A_2^{(6)} \left[\frac{m_\tau}{m_e}, \gamma\gamma \right] = 39.6 \left[\frac{\alpha}{\pi} \right]^3 = 4.96 \times 10^{-7}. \quad (121)$$

Similarly, the contribution of Fig. 19(b) is

$$A_2^{(6)} \left[\frac{m_\tau}{m_\mu}, \gamma\gamma \right] = 4.47 \left[\frac{\alpha}{\pi} \right]^3 = 5.60 \times 10^{-8}. \quad (122)$$

Thus we obtain the total contribution

$$(a_\tau - a_e)^{(6)}(\gamma\gamma) = 5.52 \times 10^{-7}. \quad (123)$$

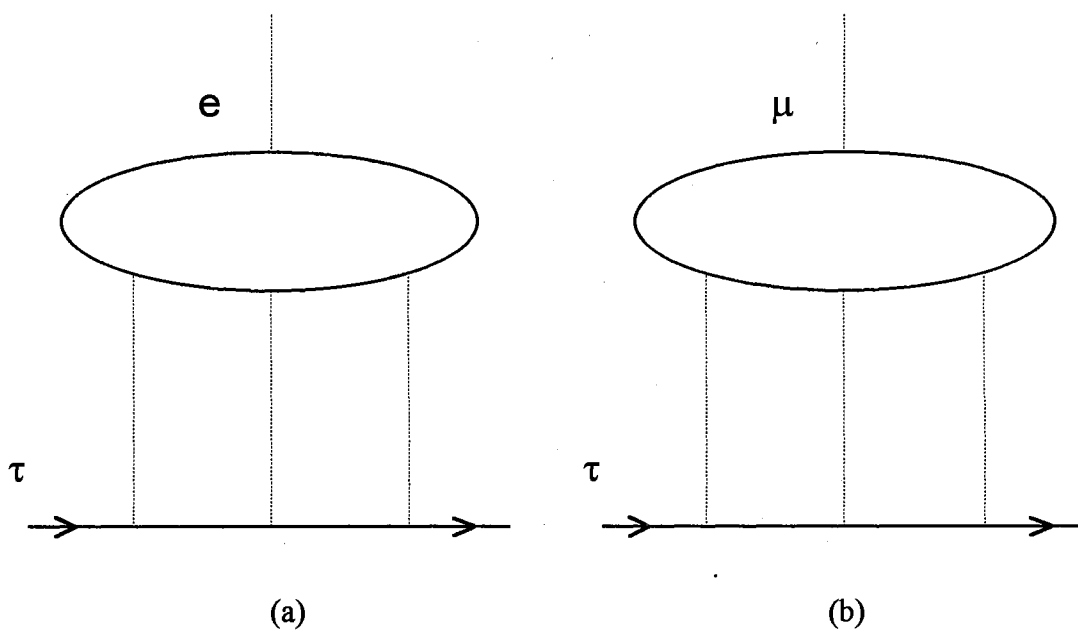


Figure 19. Sixth-order light-by-light scattering diagrams contributing to the tau anomaly

The sixth-order vacuum polarization (vp) contribution can be obtained by replacing (m_μ/m_e) by (m_τ/m_e) in the Eqs. (31)-(59) and is given by

$$A_2^{(6)} \left[\frac{m_\tau}{m_e}, \text{vp} \right] = 7.2670 \left[\frac{\alpha}{\pi} \right]^3 = 9.11 \times 10^{-8}. \quad (124)$$

Similarly we obtain

$$A_2^{(6)} \left[\frac{m_\tau}{m_\mu}, \text{vp} \right] = -0.1222 \left[\frac{\alpha}{\pi} \right]^3 = -1.53 \times 10^{-9} \quad (125)$$

and

$$A_3^{(6)} \left[\frac{m_\tau}{m_e}, \frac{m_\tau}{m_\mu} \right] = 1.679 \left[\frac{\alpha}{\pi} \right]^3 = 2.1 \times 10^{-8}. \quad (126)$$

Thus the total vp contribution is

$$(a_\tau - a_e)^{(6)} (\text{vp}) = 1.11 \times 10^{-7} \quad (127)$$

and the total sixth order contribution is given by

$$(a_\tau - a_e)^{(6)} = 6.63 \times 10^{-7}. \quad (128)$$

We will use

$$(a_\tau - a_e)^{(6)} = 6.6(1) \times 10^{-7}. \quad (129)$$

This gives us, for the QED contribution,

$$a_\tau^{\text{QED}} - a_e^{\text{QED}} = 1.354(1) \times 10^{-5} \quad (130)$$

and using the result for a_e given by Eq. (26) we obtain

$$a_\tau^{\text{QED}} = 117.319(1) \times 10^{-5}. \quad (131)$$

Because of the large mass scale m_τ the hadronic contribution $a_\tau(\text{hadronic})$ and the weak-interaction contribution $a_\tau(\text{weak})$ are significant. As we shall see the accuracy of our result will be limited by the error estimate for $a_\tau(\text{hadronic})$.

The best way to calculate $a_\tau(\text{hadronic})$ is to make use of the experimental cross section $\sigma_H(e^+e^- \rightarrow \text{hadrons})$ from threshold to high energies. We follow the methods of Refs. [54] and [53] and use the equation [63]

$$a_\tau(\text{hadronic}) = \frac{1}{4\pi^3} \int_{4m_\pi^2}^{\infty} \sigma_H(s) k_\tau(s) ds, \quad (132)$$

where $k(s)$ is known explicitly and can be found in Ref. [63].

The dominant contribution comes from the ρ resonance. We use a Breit-Wigner formalism to obtain this contribution:

$$a_\tau(\rho) = 1.88 \times 10^{-6}. \quad (133)$$

Adding the contributions from the ω , ϕ , and ψ and the continuum we obtain our result

$$a_\tau^{\text{vac}}(\text{hadronic}) = 3.6(3)(1) \times 10^{-6}. \quad (134)$$

The first error comes from taking the absolute upper and lower bounds of the contribution to a_τ^{vac} corresponding to each continuum contribution to a_τ^{vac} in Ref. [63], Table III, while the second error comes from the error in the experimental cross section σ_H . Adding our estimate for the higher-order hadronic contribution

$$a_\tau(\text{HH}) = -1.2(2) \times 10^{-7}, \quad (135)$$

we obtain our final result

$$a_\tau(\text{hadronic}) = 3.5(3)(1) \times 10^{-6}. \quad (136)$$

As a check, the hadronic contribution is estimated by inserting quarks in place of the electron in the diagram of Fig. 18(a). We use $a_\tau(\text{hadronic})$ to determine the masses

of the quarks. The result is rather insensitive to m_e and m_s . We then insert these quark masses in Fig. 18(a) obtaining our result for a_τ (hadronic). We obtain

$$a_\tau(\text{hadronic}) = 2.6 \times 10^{-6}. \quad (137)$$

This result, which is not accurate due to unknown systematic errors, is about 25% below our result in Eq. (136). We will use the result in Eq. (136) which should be a reliable value for a_τ (hadronic) because the quoted error was estimated by using absolute upper and lower bounds.

The weak-interaction contribution is easily obtained by scaling the corresponding contribution for the muon

$$a_\tau(\text{weak}) = \left(\frac{m_\tau}{m_\mu} \right)^2 a_\mu(\text{weak}) = 5.560(2) \times 10^{-7}. \quad (138)$$

Finally, adding the results of Eqs. (131), (136), and (138) we obtain our result

$$a_\tau = 11773(3) \times 10^{-7}, \quad (139)$$

or

$$g_\tau = 2.0023556(6). \quad (140)$$

It can be seen that the error in a_τ (hadronic) is comparable to the sixth order contribution and the weak contribution and dominates the error in a_τ . We note that a_τ (hadronic) is about 50 times larger than a_μ (hadronic). A measurement accurate enough to see a_τ (hadronic) would be very interesting. Of course, first a measurement to verify that $g_\tau \approx 2$ is necessary. If one would measure a_τ directly as in the case of the muon and the electron, then a measurement with an accuracy of only 3 parts per 10^3 would allow one to see the hadronic contribution. The present bound for a_τ is given by [64,65]

$$|a_\tau^{\text{exp}}| < 0.11.$$

The experimental accuracy will improve in the future reaching $\pm 4 \times 10^{-5}$ at the CERN Large Hadron Collider (LHC) if heavy-ion collisions are possible.

CHAPTER V

PADÉ APPROXIMANT METHOD

General Definition

Padé approximant (PA) is a mathematical method which can be used to accelerate convergence of an infinite series.

Let $f(x)$ be an analytic function defined by its Taylor series

$$f(x) = \sum_{n=0}^{\infty} r_n x^n . \quad (142)$$

The Padé approximant to the function $f(x)$ is defined as [68,69,70,71,72,73,74]

$$f^{(n,m)}(x) = \frac{P_n(x)}{Q_m(x)} = f(x) + O(x^{n+m+1}) , \quad (143)$$

where $P_n(x)$ and $Q_m(x)$ are polynomials of degree n and m , respectively:

$$P_n(x) = a_0 + a_1 x + a_2 x^2 + \dots + a_n x^n , \quad (144)$$

$$Q_m(x) = 1 + b_1 x + b_2 x^2 + \dots + b_m x^m , \quad (145)$$

here we have taken $b_0 = 1$ without loss of generality.

Once the coefficients a_i ($i = 0..n$) and b_j ($j = 1..m$) are determined from Eq.(143), then the Padé approximant to the series will be given by

$$f(x) \approx \frac{P_n(x)}{Q_m(x)} = \frac{a_0 + a_1 x + \dots + a_n x^n}{1 + b_1 x + \dots + b_m x^m} . \quad (146)$$

It is easy to find that the coefficients a_i and b_j are given by

$$a_i = \sum_{l=|i-m|}^i r_l b_{i-l} \quad (i = 0, 1, \dots, n) , \quad (147)$$

$$\sum_{k=0}^m r_{j-k} b_k = 0 \quad (j = n+1, n+2, \dots, n+m), \quad (148)$$

where we define

$$\|i - m\| = \frac{|i - m| + i - m}{2} = \begin{cases} 0 & (\text{if } i \leq m) \\ i - m & (\text{if } i > m) \end{cases}. \quad (149)$$

In applying Eqs. (147) and (148), it should be noted that $b_0 = 1$ and $r_k = 0$ for all $k < 0$.

Padé approximants can also be used to approximate a specific term in a series. For the Padé approximant $f^{(n,m)}(x)$, the next term which can be approximated is r_{n+m+1} and is given by

$$r_{n+m+1} \approx -(b_1 r_{n+m} + b_2 r_{n+m-1} + \dots + b_m r_{n+1}) = -\sum_{k=1}^m b_k r_{n+m+1-k}. \quad (150)$$

This is very useful since for most series encountered in physics we only know the first few terms. By using Padé approximants we can predict the next term in terms of the previous few terms. It is interesting to note that the next term predicted is independent of both x and the coefficients a_i and is dependent only on the previous terms and the coefficients b_j .

To illustrate the use of Padé approximant method, we give a very simple example:

Let

$$f(x) = \ln(1+x) = 0 + x - \frac{x^2}{2} + \frac{x^3}{3} - \frac{x^4}{4} + \dots \quad (151)$$

and suppose we know this series only up to the term $-x^4/4$. Now we try to use the Padé approximant method to approximate this series and also to predict the next term.

Since the last term we know corresponds to $n+m=4$, we can use $(n,m) = (1,3)$, $(3,1)$, or $(2,2)$. For example, taking $n=m=2$ we have

$$f^{(2,2)}(x) = \frac{P_2(x)}{Q_2(x)} = \frac{a_0 + a_1 x + a_2 x^2}{1 + b_1 x + b_2 x^2} = x - \frac{x^2}{2} + \frac{x^3}{3} - \frac{x^4}{4} + O(x^5). \quad (152)$$

The coefficients can be found by using Eqs. (147) and (148) with $r_0 = 0$, $r_1 = 1$, $r_2 = -1/2$, $r_3 = 1/3$, and $r_4 = -1/4$:

$$\begin{aligned} a_0 &= 0 \\ a_1 &= 1 \\ a_2 &= b_1 - \frac{1}{2} \\ \frac{1}{3} - \frac{b_1}{2} + b_2 &= 0 \\ -\frac{1}{4} + \frac{b_1}{3} - \frac{b_2}{2} &= 0 \end{aligned} \tag{153}$$

which gives

$$f^{(2,2)}(x) = \frac{P_2(x)}{Q_2(x)} = \frac{x + \frac{x^2}{2}}{1 + x + \frac{x^2}{6}} \tag{154}$$

Taking $x = 1$ will leads to

$$f^{(2,2)}(1) = \frac{9}{13} \approx 0.6923 \tag{155}$$

The next term predicted by the Padé approximant is r_5 which is given by

$$r_5 \approx -(b_1 r_4 + b_2 r_3) = \frac{1}{4} - \frac{1}{3} \times \frac{1}{6} \approx 0.1944 \tag{156}$$

The other Padé approximants, $f^{(1,3)}(1)$ and $f^{(3,1)}(1)$, can similarly be found. We list all our results and the comparisons with the exact result and the partial sum in Table II. From the table we see that the diagonal Padé approximant $f^{(2,2)}(1)$ gives the more accurate approximation. This is generally true for most series.

We have written a computer program [see Appendix B] which uses the Eqs. (147), (148) and (150) to approximate any arbitrary series and also predict the coefficient of the next term r_{n+m+1} . Some illustrative results are presented in Table III. It can be seen that

the Padé approximant method predicts the next coefficient very accurately, with the accuracy of the prediction increasing as n and m increase.

It is interesting to note that for a geometric series or the sum of several geometric series with various sign patterns the Pade approximant method gives the exact result after a few terms. For a series with a complicated sign pattern, the Padé approximant can also give a very good estimate.

PA Applications to the Anomaly Series

We now turn to the application of Padé approximants to perturbation series of the anomalous magnetic moments of the electron, the muon, and the tau we discussed in the previous chapters. As we will see, the Padé approximant method works best for higher-order terms. But this is just where good estimates are badly needed, since higher-order contributions involve hundreds of Feynman diagrams and the computations are extremely complicated.

We begin with the difference between the muon and the electron anomalous magnetic moments (only QED contribution).

$$a_\mu - a_e = 1.094x^2 + 22.87x^3 + 127x^4 + 570x^5, \quad (157)$$

where $x = \alpha/\pi$. The results are given in Table IV. It can be seen that there is good agreement with the known results. Moreover the next term is predicted to be about 2500 and this agrees very well with the estimate from the Kinoshita Method

$$a_\mu^{(12)} = 10k^3 a_\mu^{(6)}(\gamma\gamma) = 2500(900), \quad (158)$$

where we take $2 \leq k \leq 2.5$ (see Kinoshita, Nizic and Okamoto [6] for a discussion of this method). For the next-next term, we estimate, using the same range for k ,

$$a_\mu^{(14)} = 15k^4 a_\mu^{(6)}(\gamma\gamma) = 12500(7500). \quad (159)$$

The average values are 2460 for the next term and 10565 for the next-next term.

Next we consider the anomalous magnetic moment of the electron.

$$a_e = 0.5x - 0.3285x^2 + 1.1765x^3 - 1.43x^4 . \quad (160)$$

The results are given in Table V. From the table we see that the Padé approximant $[0,2] = -1.40$ is in an excellent agreement with the exact value for the third term $r_3 = -1.43$. The average values are 2.6 for the next term and -4.6 for the next-next term. It is interesting to note that the sign pattern (oscillating series) is kept by the Padé method.

We now consider the anomalous magnetic moment of the muon given by

$$a_\mu = 0.5x + 0.7655x^2 + 24.05x^3 + 125.6x^4 + 573(140)x^5 . \quad (161)$$

The results are shown in Table VI. The Padé prediction for the coefficient of x^5 is 656 and is very close to the known result 573. The predictions for the next and next-next terms agree very well with the estimates using the Kinoshita Method.

Lastly we consider the difference between the anomalous magnetic moments of the tau and the electron given by

$$a_\tau - a_e = 2.39x^2 + 52.9x^3 + 325x^4 + 1779x^5 \\ + 8125x^6 + 33400x^7 . \quad (162)$$

where the last four terms (eighth-, tenth-, twelfth-, and fourteenth-order terms) are estimated by using Kinoshita's method as mentioned above. The predictions from Padé approximant method are listed in Table VII, together with the comparison with the results from Kinoshita's method. We see that two results are again in good agreement.

TABLE II

PADÉ APPROXIMANTS TO THE SERIES $\ln(1+x)$ WITH $x = 1$

	Whole Series		Next Term	
	Value	%error	Value	%error
Partial Sum	$1 - \frac{1}{2} + \frac{1}{3} - \frac{1}{4} = 0.5833$	15.8	-----	-----
Exact Result	$\ln(2) = 0.6931$	-----	0.2	-----
$f^{(1,3)}(1)$	0.6857	1.07	0.1736	13.2
$f^{(3,1)}(1)$	0.6905	0.38	0.1875	6.3
$f^{(2,2)}(1)$	0.6923	0.12	0.1944	2.8

TABLE III

PADÉ APPROXIMANT TO SOME KNOWN SERIES

SERIES	$[N,M]=f^{(n,m)}$	ESNT	EXACT
$\sum_{k=0}^{\infty} \frac{x^k}{k!} = e^x$ with $x = 1$	[2,1]	0.0556	0.0417
$\sum_{k=1}^{\infty} \frac{1}{k^2}$	[3,2]	0.0202	0.0204
	[10,8]	0.002499999996	0.0025
	[15,13]	0.0011111111111111	0.0011111111111111
$\sum_{k=1}^{\infty} \frac{(-1)^k}{k^4}$	[2,1]	-0.0012	-0.0016
	[6,4]	4.821×10^{-5}	4.823×10^{-5}
	[10,8]	$6.24999987 \times 10^{-6}$	6.25×10^{-6}
$4 \sum_{k=1}^{\infty} \frac{(-1)^{k+1}}{2k-1}$	[3,2]	0.306	0.308
	[6,4]	-0.173911	-0.173913
	[10,8]	-0.10256410253	-0.10256410256
$\sum_{k=1}^{\infty} \frac{1}{4k^2-1}$	[15,13]	$2.7785495970 \times 10^{-4}$	$2.7785495971 \times 10^{-4}$
$\sum_{k=1}^{\infty} \frac{1}{k^4}$	[10,9]	$5.14189044 \times 10^{-6}$	$5.14189047 \times 10^{-6}$
$\sum_{k=0}^{\infty} \frac{1}{2^k k^4}$	[10,9]	$2.45184443 \times 10^{-12}$	$2.45184444 \times 10^{-12}$
$\sum_{k=1}^{\infty} \frac{1}{k(k+1)(k+2)}$	[10,9]	$9.410878970 \times 10^{-5}$	$9.410878976 \times 10^{-5}$

ESNT : Estimated Next Term.

TABLE IV

PADÉ APPROXIMANT TO $a_\mu - a_e$

[N, M]	ESTIMATE	KNOWN RESULT
[1, 1]	705	570
[1, 2]	2362	2500(900) NT
[2, 1]	2558	2500(900) NT
[1, 3]	9435 ($r_4 = 2362$)	12500(7500) NNT
[2, 2]	9435 ($r_4 = 2362$)	12500(7500) NNT
[3, 1]	9788 ($r_4 = 2362$)	12500(7500) NNT
[1, 3]	11771 ($r_4 = 2558$)	12500(7500) NNT
[2, 2]	11480 ($r_4 = 2558$)	12500(7500) NNT
[3, 1]	11480 ($r_4 = 2558$)	12500(7500) NNT

NT : next term

NNT : next next term.

TABLE V
PADÉ APPROXIMANT TO a_e

[N, M]	ESTIMATE	KNOWN RESULT
[1, 1]	-4.21	-1.43
[0, 2]	-1.40	-1.43
[1, 2]	3.22	NT
[2, 1]	1.74	NT
[2, 2]	-2.12 ($r_4=1.74$)	NNT
[3, 1]	-2.12 ($r_4=1.74$)	NNT
[1, 3]	-4.93 ($r_4=3.22$)	NNT
[2, 2]	-4.93 ($r_4=3.22$)	NNT
[3, 1]	-7.25 ($r_4=3.22$)	NNT

NT : next term

NNT : next next term.

TABLE VI
PADÉ APPROXIMANT TO a_μ

[N, M]	ESTIMATE	KNOWN RESULT
[2, 1]	656	573
[2, 2]	2548	2500(900) NT
[3, 1]	2614	2500(900) NT
[2, 3]	11270 ($r_s = 2548$)	12500(7500) NNT
[3, 2]	11270 ($r_s = 2548$)	12500(7500) NNT
[4, 1]	11330 ($r_s = 2548$)	12500(7500) NNT
[2, 3]	11972 ($r_s = 2614$)	12500(7500) NNT
[3, 2]	11925 ($r_s = 2614$)	12500(7500) NNT
[4, 1]	11925 ($r_s = 2614$)	12500(7500) NNT

NT : next term

NNT : next next term.

TABLE VII

PADÉ APPROXIMANT TO $a_r - a_e$

ORDER	PADÉ METHOD		KINOSHITA METHOD
	[N,M]		
10	[1, 1]	1997	1779
12	[1, 2]	9536	8125
	[2, 1]	9738	
	AVE	9637	
14	[1, 3]	32992	33400
	[2, 2]	23695	
	[3, 1]	37108	
	AVE	31265	

AVE : average value.

BIBLIOGRAPHY

1. J. E. Nafe, E. B. Nelson, and I. I. Rabi, Phys. Rev. 71, 914(1947); D. E. Nagle, R. S. Julian, and J. R. Zacharias, Phys. Rev. 72, 971(1947).
2. W. E. Lamb and R. C. Retherford, Phys. Rev. 72, 241(1947).
3. J. Schwinger, Phys. Rev. 76, 790(1949).
4. M. E. Cage *et al.*, IEEE Trans. Instrum. Meas. 38, 284(1989).
5. T. Kinoshita and W. J. Marciano, in Quantum Electrodynamics (see Ref. [36]), p. 419.
6. T. Kinoshita, B. Nizic, and Y. Okamoto, Phys. Rev. D41, 593(1990).
7. E. R. Cohen and B. N. Taylor, Rev. Mod. Phys. 59, 1121(1987).
8. R.S. Van Dyck, Jr., P.B. Schwinberg, and H. G. Dehmelt, Phys. Rev. Lett. 59, 26(1987).
9. R. Karplus and N. M. Kroll, Phys. Rev. 77, 536(1950).
10. C. M. Sommerfield, Phys. Rev. 107, 328(1957).
11. A. Petermann, Helv. Phys. Acta 30, 407(1957); Nucl. Phys. 3, 689(1957).
12. M. J. Levine and J. Wright, Phys. Rev. D8, 3171(1973).
13. P. Cvitanovic and T. Kinoshita, Phys. Rev. D10, 4007(1974).
14. R. Carroll and Y. P. Yao, Phys. Lett. 48B, 125(1974).
15. R. Carroll, Phys. Rev. D12, 2344(1975).
16. M. J. Levine and R. Roskies, Phys. Rev. D9, 421(1974).
17. M. J. Levine, R. C. Perisho and R. Roskies, Phys. Rev. D13, 997(1976).
18. M. J. Levine and R. Roskies, Phys. Rev. D14, 2191(1976).
19. K. A. Milton, W. Tsai and L. L. DeRaad Jr., Phys. Rev. D9, 1809(1974).
20. K. A. Milton, W. Tsai and L. L. DeRaad Jr., Phys. Rev. D9, 1814(1974).

21. R. Barbieri, M. Caffo, and E. Remiddi, Phys. Lett. B57, 460(1975).
22. J. A. Mignaco and E. Remiddi, Nuovo Cimento A60, 519(1969).
23. D. Billi, M. Caffo and E. Remiddi, Nuovo Cimento Lett. 4, 657(1972).
24. R. Barbieri, M. Caffo and E. Remiddi, Nuovo Cimento Lett. 5, 769(1972).
25. R. Barbieri, M. Caffo and E. Remiddi, Nuovo Cimento Lett. 9, 690(1974).
26. R. Barbieri and E. Remiddi, Phys. Lett. B49, 468(1974).
27. R. Barbieri, M. Caffo, E. Remiddi, S. Turrini and D. Oury, Nucl. Phys. B144, 329(1978).
28. T. Kinoshita, IEEE Trans. Instrum. Meas., 38, 172(1989).
29. T. Kinoshita and W. B. Lindquist, Phys. Rev. D27, 867(1983).
30. T. Kinoshita and W. B. Lindquist, Phys. Rev. D27, 877(1983).
31. T. Kinoshita and W. B. Lindquist, Phys. Rev. D27, 886(1983).
32. T. Kinoshita and W. B. Lindquist, Phys. Rev. D39, 2407(1989).
33. B. Lautrup, Phys. Lett. B69, 109(1977); M. A. Samuel, Nuovo Cimento Lett., 21, 227(1978); M. Caffo, S. Turrini, and E. Remiddi, Nuclear Phys. B141, 302(1978); M. L. Laursen and M. A. Samuel, Oklahoma State University preprint (1979).
34. C. Itzykson, G. Oarisi, and J.-B. Zuber, Phys. Rev. D16, 996(1977).
35. T. Kinoshita, New Frontiers in High Energy Physics, Eds., B.Kursunoglu, A. Perlmutter, and L. F. Scott (Plenum, New York, 1978), pp.127-143.
36. J. Bailey *et al.*, Phys. Lett. 68B, 191(1977); F. J. M. Farley and E. Picasso, in Quantum Electrodynamics, edited by T. Kinoshita (World Scientific, Singapore, 1990), p. 479.
37. H. H. Elend, Phys. Lett. 20, 682(1966).
38. K. Mitchell, Phil. Mag. 40/I 351(1949).
39. T. Kinoshita, Phys. Rev. D40, 1323(1989).
40. M. A. Samuel, Oklahoma State University Research Report No. 255, 1991.

41. J. Aldins, S. J. Brodsky, A. Dufner, and T. Kinoshita, Phys. Rev. Lett. 23, 441 (1969); Phys. Rev. D1, 2378(1970).
42. M. A. Samuel and C. Chlouber, Phys. Rev. Lett. 36, 442(1976).
43. R. Barbieri, E. Remiddi, Nucl. Phys. B90, 233(1975).
44. B. E. Lautrup and E. de Rafael, Phys. Rev. 174, 1835(1968).
45. S. J. Brodsky and E. de Rafael, Phys. Rev. 168, 1620(1968).
46. M. A. Samuel, Nucl. Phys. B70, 351(1974).
47. M. L. Laursen, M. A. Samuel, and A. K. Ray, Z. Phys. C6, 3(1980).
48. M. Laursen and M. A. Samuel, Phys. Rev. D19, 1282(1979).
49. C. Chlouber and M. A. Samuel, Phys. Rev. D17, 2817(1978).
50. We use Kinoshita's improved results which he obtained in a recent recalculation of diagrams 13(a)-13(d). These results differ from the published values in Refs. [5] and [6]. See Muon g-2: Theory, in the Proceedings of the Workshop on the Future of Muon Physics, Heidelberg, Germany, 1991.
51. J. Aldins, S. J. Brodsky, A. Dufner, and T. Kinoshita, Phys. Rev. Lett. 23, 441 (1969); Phys. Rev. D1, 2378(1970).
52. C. Chlouber and M. A. Samuel, Phys. Rev. D16, 3596(1977).
53. T. Kinoshita, B. Nizic, and Y. Okamoto, Phys. Rev. D31, 2108(1985).
54. L. Martinovic and S. Dubnicka, Phys. Rev. D42, 884(1990).
55. This is very important, in the light of the new BNL experiment, to calculate the two-loop weak contribution. This is being done by E. Kuraev of Novosibirisk, U.S.S.R. .
56. S. Laporta and E. Remiddi, Phys. Lett. B301, 440(1993).
57. M. L. Perl et al., Phys. Rev. Lett. 35, 1489(1975).
58. For a recent review, see M. L. Perl, in Proceedings of the 1989 International Symposium on Lepton and Photon Interactions at High Energy, Stanford, 7-12 August 1989, edited by Michael Riordan (World Scientific, Singapore, 1990).
59. M. L. Laursen, M. A. Samuel, and A. Sen, Phys. Rev. D29, 2652(1984).

60. M. L. Perl, in Proceedings of the Lake Louise Winter Institute, February 1991.
61. I. J. Kim, Nucl. Phys. B229, 251(1983).
62. D. Chen *et al*, Phys. Rev. Lett. 69, 3286(1992).
63. See also J. A. Casas, G. Lopez, and F. J. Yndurain, Phys. Rev. D32, 736(1985).
64. J. A. Grifols and A. Mendez, Phys. Lett. B255,611(1991).
65. F. Del Aguila, F. Cornet, and J. I. Illana, Phys. Lett. B271, 256(1991).
66. We thank T. Kinoshita for making his new results available to us.
67. T. Kinoshita, Z. Phys. C56 (Supplements), 13(1992).
68. C. Chlouber, G. W. Li and M. A. Samuel, Oklahoma State university Research Note 265, February (1992).
69. M. A. Samuel, G. W. Li and E. Steinfelds, Phys. Rev. D48, 869(1993).
70. M. A. Samuel and G. W. Li, SLAC-PUB-6370 (1993).
71. M. A. Samuel and G. W. Li, SLAC-PUB-6318 (1993).
72. M. A. Samuel and G. W. Li, Oklahoma State University Research Note 275, International Journal of Theoretical Phys.(1994).
73. M. A. Samuel, G. W. Li and E. Steinfelds, Oklahoma State University Research Note 273, Phys. Lett. (1994).
74. M. A. Samuel, G. W. Li and E. Steinfelds, Oklahoma State University Research Note 278 (1994).

APPENDIX A

COMPARISON BETWEEN OUR RESULTS AND KINOSHITA'S RESULTS IN THE FOURTH AND SIXTH ORDER QED CONTRIBUTIONS

So far the QED contribution to the anomaly of the muon, a_μ , has been calculated and estimated up to the tenth order. In this endeavor, Kinoshita has made a great contribution. However, we find that our results and Kinoshita's results in fourth and sixth order are slightly different, for some contributions. In this appendix, we will present this comparison in some detail.

A-1 Comparison in the Fourth Order Contribution

For the fourth order contribution, differences occur in the calculations of $A_2^{(4)}(m_\mu/m_e)$ and $A_2^{(4)}(m_\mu/m_\tau)$ terms. For the $A_2^{(4)}(m_\mu/m_e)$ term, Kinoshita just kept terms up to the second order in (m_μ/m_e) and got the result

$$A_2^{(4)} \left[\frac{m_\mu}{m_e} \right] = 1.0942596. \quad (\text{A1})$$

In fact, the contributions from the third order and even the fourth order terms should be taken into account. For the $A_2^{(4)}(m_\mu/m_\tau)$ term, Kinoshita's result is

$$A_2^{(4)} \left[\frac{m_\mu}{m_\tau} \right] = 7.794(32) \times 10^{-5}. \quad (\text{A2})$$

To the accuracy required, we agree on the quantity $A_2^{(4)}(m_e/m_\mu)$ which is to be subtracted. Kinoshita's value is

$$A_2^{(4)} \left[\frac{m_e}{m_\mu} \right] = 5.198 \times 10^{-7}. \quad (\text{A3})$$

Our values are given in Eqs. (39), (40), and (41). These should be compared with Kinoshita's results in Eqs. (A1), (A2), and (A3), respectively. Thus the total difference in the fourth order contribution is given by $\Delta_1 = -7 \times 10^{-12}$. (A4)

A-2 Comparison in the Sixth Order Contribution

We find that our results, corresponding to each subgroup of $A_2^{(6)}(m_\mu/m_e)$, are somewhat different from those of Kinoshita. For the vacuum-polarization part, the diagrams in Fig. 13, the results are listed in Table I.

In the table, Δ' is the difference between our results, without the m_e/m_μ and smaller terms, and Kinoshita's results. It is clear that these terms improve the agreement with Kinoshita's results and are definitely necessary at this level of precision.

As seen, the total difference is given by

$$\Delta_2 = -1(6) \times 10^{-12}. \quad (\text{A5})$$

As stated above, this difference reflects the uncertainty coming from the uncalculated terms in our analytical calculations and the uncertainty in the numerical integrations in Kinoshita's results.

The other difference in the sixth order comes from Kinoshita's neglect of the contributions from τ . The contributions due to Fig. 12 with $e \rightarrow \tau$ and Figs. 14 and 15 are given in Table VIII. We see that the total result turns out to be relatively small due to the cancellation which occurs.

Collecting all the differences from the fourth- and the sixth-order contributions, as well as the one from $\alpha_e^{\text{hadronic}}$, we get the total QED difference given by

$$\Delta\alpha^{\text{QED}} = -12 \times 10^{-12}, \quad (\text{A6})$$

which is just the one given by Eq. (98). These are Kinoshita's new results, obtained after an error was discovered [66] in his earlier results. His new results were published in ref [67].

TABLE VIII

CONTRIBUTIONS TO $A_2^{(6)}(m_\mu/m_\tau, \gamma\gamma)$ AND $A_2^{(6)}(m_\mu/m_\tau, \nu\bar{\nu})$

Figure	Contribution (10^{-3})	$\Delta(\alpha/\pi)^3$ (10^{-12})
12(with $e \rightarrow \tau$)	1.836	23.0
14	-2.063	-25.9
15	0.2959	3.7
Total	0.0689	0.86

APPENDIX B

Padé approximant FORTRAN program

```

*****
*
*   This program is used to calculate any arbitrary series and also estimate
*   a specific term of the series by using the Padé approximant method.
*
*   The series takes the following form:
*        $f(x)=r(0)+r(1)x+r(2)x^{**2}+...+r(n+m)x^{**n+m}+O(x^{**n+m+1})$ 
*   The Padé approximant to this series is given by
*        $p(n,m)=P(n)/Q(m)$ 
*   where
*        $P(n)=a(0)+a(1)x+a(2)x^{**2}+...+a(n)x^{**n}$ 
*        $Q(m)=1+b(1)x+b(2)x^{**2}+...+b(m)x^{**m}$ 
*   and the next term to be predicted is the coefficient  $r(n+m+1)$ .
*
*****

      IMPLICIT REAL *8 (A-H,O-Z)
      DIMENSION R(0:100)
      X = 1.0D0
c  Assign values to r(i) (i=1,nn)
      NN = 4                                ! nn=n+m
      R(0) = 0.0D0
      R(1) = 1.0D0
      R(2) = -0.5D0
      R(3) = 1.0D0/3.0D0
      R(4) = -0.25D0

      DO 10 N =1, NN-1
      M = NN-N
      CALL PADE(N,M,X,R,TERM,PA)
      WRITE(*,20)N,M,TERM,R(NN+1),PA
20  FORMAT(1X,'(,I2,1X,I2,)'=,D30.22/1X,'EXACT =',D30.22,
1     /1X,'PADE = ',D30.22)
10  CONTINUE
      STOP
      END
*****

*   Subroutine of Padé approximant
*   Input parameters:
*       N, M ----- As in P(N,M).
*       X ----- The variable x.
*       R ----- The coefficients of the series.
*   Output arguments:
*       TERM ---- The estimation to the next term.
*       PA ----- The approximation to the whole series.
*****

```

```

SUBROUTINE PADE(N,M,X,R,TERM,PA)
IMPLICIT REAL *8 (A-H,O-Z)
DIMENSION A(0:50),B(50),AUG(50,51),R(0:100)
COMMON B

```

c Assign values to the augmented matrix aug(i,j) used to solve for b(j).

```

DO 30 I = 1,M
DO 30 K = 1,M-I
AUG(K,K+I) = -R(N-I)
30 CONTINUE
DO 40 I = 0,M-1
DO 40 K = I+1, M
AUG(K,K-I) = -R(N+I)
40 CONTINUE
DO 50 K=1, M
AUG(K,M+1) = R(N+K)
50 CONTINUE

```

```
CALL GAUSS(AUG,M)
```

c Solve for a(k) (k=1,n)

```

IF(N. GE .M) THEN
A(0) = R(0)
DO 60 K = 1, M
A(K) = R(K)
DO 60 I = 1, K
60 A(K) = A(K)+B(I)*R(K-I)
DO 70 K = M+1, N
A(K) = R(K)
DO 70 I = 1, M
70 A(K) = A(K)+B(I)*R(K-I)
ELSE
A(0) = R(0)
DO 80 K = 1,N
A(K) = R(K)
DO 80 I = 1,K
80 A(K) = A(K)+B(I)*R(K-I)
ENDIF

```

c Find the result p(n,m)

```

AA = 0.0D0
DO 90 J = 0,N
90 AA = AA+A(J)*X**J
BB = 1.0D0
DO 100 J = 1, M

```

```

100  BB = BB+B(J)*X**J
      PA = AA/BB                               ! this is p(n,m)

c    Estimate the next term
      TERM = 0.0D0
      DO 110 I = 1, M
110   TERM = TERM-B(I)*R(N+M+1-I)             ! this is r(n+m+1)
      RETURN
      END

*****
*   Subroutine to solve N linear equations by using Gaussian Elimination   *
*   method.                                                                *
*       N   ----- The number of equations                               *
*       AUG ----- The augmented matrix                                  *
*       XX  ----- The solutions                                         *
*****

      SUBROUTINE GAUSS(AUG,N)
      IMPLICIT REAL *8 (A-H,O-Z)
      DIMENSION AUG(50,51),XX(50)
      COMMON XX
      L = 1
      DO WHILE(L .LT. N)
      CALL PIVOT(AUG,N,L)
      REV = 1.0D0/AUG(L,L)
      AUG(L,L) = 1.0D0
      DO 120 K = L+1, N+1
      AUG(L,K) = AUG(L,K)*REV
120   CONTINUE
      DO 130 J = L+1, N
      XMULT = -AUG(J,L)
      AUG(J,L) = 0.0D0
      DO 140 K = L+1, N+1
      AUG(J,K) = AUG(J,K)+XMULT*AUG(L,K)
140   CONTINUE
130   CONTINUE
      L = L+1
      ENDDO
      XX(N) = AUG(N,N+1)/AUG(N,N)
      DO 150 K = N-1, 1, 1
      XX(K) = AUG(K,N+1)
      DO 160 L = K+1, N
      XX(K) = XX(K)-AUG(K,L)*XX(L)
160   CONTINUE
150   CONTINUE
      RETURN

```

```

      END
*****
*      Subroutine to perform pivoting with respect to the Lth row and the Lth      *
*      column of the augmented matrix AUG.                                     *
*      Input arguments:                                                       *
*          N ---- The number of equation.                                     *
*          L ---- The pivot row and column.                                   *
*****

      SUBROUTINE PIVOT(AUG,N,L)
      IMPLICIT REAL *8 (A-H,O-Z)
      DIMENSION AUG(50,51)

c Find maximum pivot
      XMAX = DABS(AUG(L,L))
      MAXROW = L
      DO 170 J = L+1, N
      IF(DABS(AUG(J,L)) .GT. XMAX) THEN
      XMAX = DABS(AUG(J,L))
      MAXROW = J
      ENDIF
170 CONTINUE

c swap rows
      DO 180 K = L, N+1
      TEMP = AUG(L, K)
      AUG(L, K) = AUG(MAXROW, K)
      AUG(MAXROW, K) = TEMP
180 CONTINUE
      RETURN
      END

```

VITA 2

GUOWEN LI

Candidate for the Degree of

Doctor of Philosophy

**Thesis: THE ANOMALOUS MAGNETIC MOMENTS OF THE CHARGED
LEPTONS: THE ELECTRON, THE MUON AND THE TAU**

Major Field: Physics

Biographical:

Personal Data: Born in Ying County, Shanxi Province, P.R.China, September 1, 1962, the son of Lin Li and Yulian Li.

Education: Graduated from LinQuin Senior High School, Shanxi Province, P.R.China, in July, 1979; received Bachelor of Science Degree in Physics from Shanxi University of China in September, 1983; received Master of Science degree at Shanxi University of China in July, 1986; completed the requirements for the Doctor of Philosophy Degree at Oklahoma State University in May, 1994.

Professional Experience: Instructor, Department of Physics, Shanxi University, September, 1986, to December, 1987. Research and Teaching Assistant, Department of Physics, Oklahoma State University, January, 1989 to present.